

# *Laser Vision: Lidar as a Transformative Tool to Advance Critical Zone Science*

Adrian A. Harpold\*, University of Nevada, Reno, [aharpold@email.arizona.edu](mailto:aharpold@email.arizona.edu)

Jill A. Marshall, University of Oregon, [jillm@uoregon.edu](mailto:jillm@uoregon.edu)

Steve W. Lyon, Stockholm University, [steve.lyon@natgeo.su.se](mailto:steve.lyon@natgeo.su.se)

Theodore B. Barnhart, University of Colorado, [theodore.barnhart@colorado.edu](mailto:theodore.barnhart@colorado.edu)

Beth A. Fisher, University of Minnesota, [fisherba@umn.edu](mailto:fisherba@umn.edu)

Mitchell Donovan, University of Maryland – Baltimore County, [mdonovan@umbc.edu](mailto:mdonovan@umbc.edu)

Kristen M. Brubaker, Hobart and William Smith Colleges, [brubaker@hws.edu](mailto:brubaker@hws.edu)

Christopher J. Crosby, UNAVCO, [Crosby@unavco.org](mailto:Crosby@unavco.org)

Nancy F. Glenn, Boise State University, [nancyglenn@boisestate.edu](mailto:nancyglenn@boisestate.edu)

Craig L. Glennie, University of Houston, [clglenni@central.uh.edu](mailto:clglenni@central.uh.edu)

Peter B. Kirchner, University of California, Los Angeles, [peter.b.kirchner@jpl.nasa.gov](mailto:peter.b.kirchner@jpl.nasa.gov)

Norris Lam, Stockholm University, [norris.lam@natgeo.su.se](mailto:norris.lam@natgeo.su.se)

Kenneth D. Mankoff, Woods Hole Oceanographic Institute, [kmankoff@whoi.edu](mailto:kmankoff@whoi.edu)

James L. McCreight, National Center for Atmospheric Research, [mccreigh@gmail.com](mailto:mccreigh@gmail.com)

Noah P. Molotch, University of Colorado, Boulder, [noah.molotch@colorado.edu](mailto:noah.molotch@colorado.edu)

Keith N. Musselman, University of Saskatchewan, [keith.musselman@usask.ca](mailto:keith.musselman@usask.ca)

Jon Pelletier, University of Arizona, [jon@geo.arizona.edu](mailto:jon@geo.arizona.edu)

Tess Russo, Pennsylvania State University, [russo@psu.edu](mailto:russo@psu.edu)

Harish Sangireddy, University of Texas, Austin, [hsangireddy@utexas.edu](mailto:hsangireddy@utexas.edu)

Ylva Sjöberg, Stockholm University, [ylva.sjoberg@natgeo.su.se](mailto:ylva.sjoberg@natgeo.su.se)

Tyson Swetnam, University of Arizona, [tswetnam@email.arizona.edu](mailto:tswetnam@email.arizona.edu)

Nicole West, Pennsylvania State University, [nxw157@psu.edu](mailto:nxw157@psu.edu)

\*Corresponding author: Adrian A. Harpold, [aharpold@cabnr.unr.edu](mailto:aharpold@cabnr.unr.edu)

1            *Laser Vision: Lidar as a Transformative Tool to Advance Critical Zone Science*

2    Observation and quantification of the Earth’s surface is undergoing a revolutionary change due  
3    to the increased spatial resolution and extent afforded by light detection and ranging (lidar)  
4    technology. As a consequence, lidar-derived information has led to fundamental discoveries  
5    within the individual disciplines of geomorphology, hydrology, and ecology. These disciplines  
6    form the cornerstones of Critical Zone (CZ) science, where researchers study how interactions  
7    among the geosphere, hydrosphere, and biosphere shape and maintain the “zone of life”, which  
8    extends from the top of unweathered bedrock to the top of the vegetation canopy. Fundamental  
9    to CZ science is the development of transdisciplinary theories and tools that transcend individual  
10    disciplines and inform other’s work, capture new levels of complexity, and create new  
11    intellectual outcomes and spaces. Researchers are just beginning to utilize lidar datasets to  
12    answer synergistic, transdisciplinary questions in CZ science, such as how CZ processes co-  
13    evolve over long-time scales and interact over shorter time scales to create thresholds, shifts in  
14    states and fluxes of water, energy, and carbon. The objective of this review is to elucidate the  
15    transformative potential of lidar for CZ science to simultaneously allow for quantification of  
16    topographic, vegetative, and hydrological processes. A review of 147 peer-reviewed studies  
17    utilizing lidar highlights the lag in the application of lidar for CZ studies as 38% of the studies  
18    were focused in geomorphology, 18% in hydrology, 32% in ecology, and the remaining 12% had  
19    an interdisciplinary focus. A handful of exemplar transdisciplinary studies demonstrate that well-  
20    integrated lidar observations can lead to fundamental advances in CZ science, such as  
21    identification of feedbacks between hydrological and ecological processes over hillslope scales  
22    and the synergistic co-evolution of landscape-scale CZ structure due to interactions amongst  
23    carbon, energy, and water cycles. We propose that using lidar to its full potential will require

24 numerous advances across CZ applications, including new and more powerful open-source  
25 processing tools, exploiting new lidar acquisition technologies, and improved integration with  
26 physically-based models and complementary *in situ* and remote-sensing observations. We  
27 provide a five-year vision that advocates for the expanded use of lidar datasets and highlights  
28 subsequent potential to advance the state of CZ science.

29

## 30 **1. INTRODUCTION**

31 Complex interactions among the geosphere, ecosphere, and hydrosphere give rise to present-day  
32 landforms, vegetation, and corresponding water and energy fluxes. Critical Zone (CZ) science  
33 studies these interactions in the zone extending from the top of unweathered bedrock to the top  
34 of the vegetation canopy. Understanding CZ function is fundamental for characterizing regolith  
35 formation, carbon-energy-water cycles, meteorological controls on ecology, linked surface and  
36 subsurface processes, and numerous other Earth surface processes (NRC, 2012). Improved  
37 understanding of CZ functions is thus important for quantifying ecosystem services and  
38 predicting their sensitivity to environmental change. However, CZ processes are difficult to  
39 observe because they occur over time scales of seconds to eons and spatial scales of centimeters  
40 to kilometers, and thus require diverse measurement approaches (Chorover et al., 2011). Light  
41 detection and ranging (lidar) technologies can be helpful in this regard because they generate  
42 repeatable, precise three-dimensional information of the Earth's surface characteristics.

43

44 Lidar allows for simultaneous measurements of aboveground vegetation structure and human  
45 infrastructure, as well as the topography of the earth surface, including soils, exposed bedrock,  
46 stream channels, and snow/ice. Depending on the data collection system and platform,

47 observations can be made at the landscape scale ( $>1000 \text{ km}^2$ ) and at spatial resolutions capable  
48 of capturing fine-scale processes ( $<10 \text{ cm}$ ). These unique measurement capabilities offered by  
49 lidar have the potential to help answer transdisciplinary research questions, which transcend a  
50 single discipline, capture greater complexity, and create new intellectual advances that are  
51 synergistic (across disciplines) in nature. Fundamental CZ science questions often require  
52 transdisciplinary approaches that surpass what is possible in multidisciplinary (i.e. collaborations  
53 across disciplines that pose their own questions) or interdisciplinary (i.e. collaborations where  
54 information is transferred amongst disciplines) research settings. Because lidar can characterize  
55 geomorphic, ecologic, and hydrologic processes simultaneously across a range of scales, it is  
56 uniquely suited to address questions posed by CZ research.

57

58 Lidar acquisition capabilities are increasing exponentially (Stennett, 2004; Glennie et al., 2013)  
59 and new ground-based (terrestrial laser scanning, TLS), mobile platforms (airborne laser  
60 scanning, ALS or other mobile platforms like trucks or boats), and space-based platforms  
61 (spaceborne laser scanning, SLS) are leading to increased availability of lidar datasets with CZ-  
62 relevant information content. Different lidar platforms each have their own advantages and  
63 limitations, but operate based on a similar principle by emitting and measuring the round-trip  
64 time of travel of an energy pulse (laser light) and thus, measuring and mapping distance to a  
65 target. Collection via TLS methods, for example, typically involves lidar scanners that are  
66 mounted on tripods or other fixed locations. Fixed targets surveyed with a high resolution GPS  
67 are used to georeference the lidar datasets and to composite multiple TLS scans into a single  
68 point cloud. TLS scanners are becoming more affordable and available to individual researchers  
69 and groups. Lidar collections via mobile platforms are typically performed by mounting the lidar

70 unit on an aircraft, helicopter, or vehicle that moves over the study area of interest. The aircraft  
71 must be equipped with a GPS unit and Internal Measurement Unit (IMU) to track the orientation  
72 and location of the scanner. Similar to TLS collection, ALS methods require ground targets with  
73 known GPS locations for georeferencing. Lidar collection via SLS are much less common, but  
74 have been successfully deployed on orbiting spacecraft and will become more prevalent in 2017  
75 with the planned launch of ICESat-2 (Abdalati et al., 2010). In addition to the laser system, the  
76 spacecraft must have a GPS unit and altitude determination system in order to georeference the  
77 data. Each of these lidar platforms offer specifications that can be selected and adjusted for a  
78 given science application. Throughout this review we present studies using a suite of lidar  
79 methods and highlight the advantages of each method for differing scientific purposes.

80

81 The objective of this paper is to present a five-year vision for applying lidar to advance  
82 transdisciplinary CZ research. To accomplish this, we first present the state of the science on  
83 applying lidar to disciplinary-specific research in geomorphology, hydrology, and ecology in  
84 Sections 1.1, 1.2, and 1.3, respectively. This is followed in Section 2.1 by an exploration of  
85 transdisciplinary studies that have utilized complementary lidar-derived datasets to propel CZ  
86 science beyond what is possible within disciplinary endeavors. We summarize these exemplar  
87 transdisciplinary studies with the intent to guide future research. In Section 2.2 we describe how  
88 lidar-derived information is uniquely suited to advance three CZ research topics beyond the  
89 current state of the science: 1) quantifying change detection, 2) parameterization and verification  
90 of physical models, and 3) improved understanding of CZ processes across multiple scales.  
91 These topics are limited by a set of common impediments that we outline in Section 2.3. Finally,  
92 in Section 2.4, we present a vision to advance CZ science with lidar using examples of

93 transdisciplinary research questions and provide a set of recommendations for the CZ community  
94 to increase usage and advocate for greater lidar resources over the next five years.

95

### 96 **1.1 Advances in Geomorphology Using Lidar**

97 High-resolution topographic datasets derived from lidar have greatly contributed to quantifying  
98 geomorphic change, identifying geomorphic features, and understanding ecohydrologically-  
99 mediated processes at varying scales and extents. These advances have allowed testing of  
100 geomorphic models, pattern and process recognition, and the identification of unanticipated  
101 landforms and patterns (e.g. waveforms) that were not possible using previous survey  
102 techniques. Generally, lidar information complements rather than replaces field observations,  
103 with lidar observations leading to new hypothesis and process cognition (Roering et al., 2013).  
104 Broadly, lidar technology has been useful in studying geomorphic response to extreme events  
105 such as fire and storms (e.g., Pelletier and Orem, 2014; Sankey et al., 2013; Perignon et al.,  
106 2013; Staley et al., 2014), human activities (e.g. James et al., 2009), and past climatic and  
107 tectonic forcings (e.g., Roering, 2008; Belmont, 2011; West et al., 2014). Meter and sub-meter  
108 scale time-varying processes, often derived from TLS, have been quantified in the response of  
109 point bar and bank morphodynamics (Lotsari et al., 2014) and in the formation of  
110 microtopography due to feedbacks with biota (e.g., Roering et al., 2010; Pelletier et al., 2012;  
111 Harman et al., 2014). Examples of larger scale change detection applications, typically ALS-  
112 derived, include measuring changes in stream channel pathways resulting from Holocene climate  
113 change and anthropogenic activities (e.g., Day et al., 2013; Kessler, 2012; James 2012; Belmont  
114 et al., 2011), rates of change in migrating sand dunes (Pelletier, 2013), the influence of lithology  
115 and climate on hillslope form (e.g., Marshall and Roering, 2014; Hurst et al., 2013; Perron et al.,

116 2008; West et al., 2014), and channel head formation (e.g., Pelletier et al., 2013; Pelletier and  
117 Perron, 2012; Perron and Hamon, 2012). Automated tools to identify geomorphic features (i.e.,  
118 floodplains, terraces, landslides) and transitional zones (i.e., hillslope-to-valley, floodplain-to-  
119 channel) have been used in conjunction with high-resolution elevation datasets from lidar,  
120 including Geonet 2.0 (Passalacqua et al., 2010), ALMTools (Booth et al., 2009), and TerrEX  
121 (Stout and Belmont, 2014).

122

### 123 **1.2 Advances in Hydrology Using Lidar**

124 Research utilizing lidar has advanced fundamental process understanding in snow hydrology  
125 (Deems et al., 2013), surface water hydraulics (Lane et al., 2004; Nathanson et al., 2012; Lyon et  
126 al., 2015), and land-surface-atmosphere interactions (Mitchell et al., 2011). Lidar-derived snow  
127 depths (derived by differencing snow-on and snow-off elevations) over large ( $>1 \text{ km}^2$ ) spatial  
128 extents from both ALS and TLS (Deems et al., 2013) have yielded unprecedented contiguous  
129 maps of spatial snow distributions (e.g. Fassnacht and Deems, 2006; McCreight et al., 2014) and  
130 provided new insights into underlying processes determining spatial patterns in snow cover  
131 (Trujillo et al., 2009; Kirchner et al., 2014), accumulation and ablation rates (Grunewald et al.,  
132 2010; Varhola and Coops, 2013), snow water resource planning (Hopkinson et al., 2012), and  
133 estimating the effects of forest cover and forest disturbance on snow processes (Harpold et al.,  
134 2014a). Change detection techniques have been effective for determining glacier mass balances  
135 (Hopkinson and Demuth, 2006), ice surface properties (Williams et al., 2013), and calving front  
136 movements (e.g., Arnold et al., 2006; Hopkinson et al., 2006). Prior to lidar, many of these  
137 cryospheric processes had to be investigated using single point observations or through statistical  
138 rather than deterministic analyses; the additional information derived from lidar has yielded

139 important insights that have advanced scientific understanding. High- resolution topographic  
140 information from lidar has proved important for stream channel delineation (Kinzel et al., 2013),  
141 rating curve estimation (Nathanson et al., 2012; Lyon et al., 2015), floodplain mapping and  
142 inundation (Marks and Bates, 2000; Kinzel et al., 2007), and topographic water accumulation  
143 indices (Sørensen and Seibert, 2007; Jensco et al., 2009). Lidar measurements of micro-  
144 topography shows potential for improving soil property and moisture information (e.g.,  
145 Tenenbaum et al., 2006), surface and floodplain roughness (Mason et al., 2003, Forzieri et al.,  
146 2010; Brasington et al., 2012; Brubaker et al., 2013), hydraulic dynamics and sediment transport  
147 (Roering et al., 2012; McKean et al., 2014), surface ponding and storage volume calculations (Li  
148 et al., 2011; French, 2003), and wetland delineation (e.g. Lane and D’Amico, 2010). Certain  
149 hydrological modeling fields are well poised to utilize high-resolution topography, such as  
150 movement of water in urban environments (Fewtrell et al., 2008), in-channel flow modeling  
151 (Mandlburger et al., 2009; Legleiter et al., 2011), and hyporheic exchange and ecohydraulics in  
152 small streams (e.g. Jensco et al., 2009). Finally, high-resolution, three-dimensional lidar  
153 measurements of canopy and vegetation structure (Vierling et al., 2008) have direct implications  
154 for modeling the surface energy balance (Musselman et al., 2013; Broxton et al., 2014) and  
155 evapotranspiration processes (Mitchell et al., 2011) at scales critical to increasing fidelity in  
156 physically-based models.

157

### 158 **1.3 Advances in Ecology Using Lidar**

159 Lidar-based remote sensing of vegetation communities has transformed the way ecologists  
160 measure vegetation across multiple spatial scales (e.g., Lefsky et al., 2002; Maltamo et al., 2014;  
161 Streutker and Glenn 2006). Substantial work has been undertaken using lidar to map vegetation

162 structure and biomass distributions (see reviews by Seidel et al., 2011 and Wulder et al., 2012).  
163 These include the estimation of Leaf Area Index (LAI) (Riaño et al., 2004; Richardson et al.,  
164 2009; Hopkinson et al., 2013), vegetation roughness (Strecker and Glenn, 2006; Antonarakis et  
165 al., 2010), alpine tree lines (Coops et al., 2013), and total carbon storage and sequestration rates  
166 in forest, grassland, savannahs and/or shrubland communities (Asner et al., 2012a; Baccini et al.,  
167 2012; Mascaró et al., 2011; Simard et al., 2011; Antonarakis et al., 2014). ALS has been used to  
168 characterize wildlife habitat in tree and shrub canopies (Hyde et al., 2005; Bork and Su, 2007;  
169 Vierling et al., 2008; Martinuzzi et al., 2009; Zellweger et al., 2014) and in aquatic systems  
170 (McKean et al., 2008; Wedding et al., 2008; McKean et al., 2009). ALS has been a critical tool  
171 in modeling catchment scale water-availability for vegetation at fine (Harmon et al., 2014) and  
172 broad spatial scales (Chorover et al., 2011). Radiation transmission and ray-tracing models  
173 utilizing lidar provide ecologists with better tools to quantify in-canopy and below-canopy light  
174 environments (Lee et al., 2009; Bittner et al., 2014; Musselman et al., 2013; Bode et al., 2014;  
175 Moeser et al., 2014). Additionally, ecologists are beginning to quantify the impact of vegetation  
176 on micro-topography (Sankey et al., 2010; Pelletier et al., 2012; Harmon et al., 2014), as well as  
177 larger landform processes (Pelletier et al., 2013). Broad-scale lidar data allows for quantification  
178 of patches and mosaics amongst plant functional types across landscapes (Antonarakis et al.,  
179 2010; Dickinson et al., 2014) and global forest biomass estimates (Simard et al., 2011).  
180 Ecologists have fused data from hyperspectral imaging and lidar to enable species classification  
181 for close to a decade (e.g. Mundt et al., 2006). However, new opportunities exist to link species-  
182 level detail and plant functional response through emerging technologies, including co-  
183 deployment of hyperspectral and lidar sensors (Asner et al., 2012b), and hyperspectral  
184 (supercontinuum) laser technology (Kaasalainen et al., 2007; Hakala et al., 2012). By linking

185 lidar with additional observations, researchers have begun to quantify species-level detail and  
186 plant health estimation (Cho et al., 2012; Féret and Asner, 2012; Olsoy et al., 2014) and model  
187 forest carbon fluxes (Antonarakis et al., 2014).

188

## 189 **2. Current Toolkits and Open Questions Using Lidar in CZ Science**

190 Research based on lidar-derived information accounts for substantial advances within the  
191 cornerstone CZ disciplines. However, many open questions in CZ science require linked,  
192 transdisciplinary investigations across multiple disciplines that create new intellectual spaces for  
193 scientific advancements. For example: How do CZ processes co-evolve over long-time scales  
194 and interact over shorter time scales to develop thresholds and shifts in states and fluxes of  
195 water, energy, and carbon? What will be the response of the CZ structure to disturbance and land  
196 use change? These CZ science questions must elucidate feedbacks and interactions among the  
197 geosphere, ecosphere, and hydrosphere. This cannot be accomplished within the individual  
198 disciplines (multidisciplinary) or by sharing information across disciplines (interdisciplinary),  
199 but instead require synergistic transdisciplinary science that spans multiple spatial and temporal  
200 scales.

201

202 A key advantage of lidar for understanding CZ feedbacks is the coupling of previously  
203 unprecedented coverage over both broad temporal and spatial scales (Figure 1). The utility of  
204 lidar for geosphere, ecosphere, and hydrosphere investigations is dependent on the platform (e.g.  
205 TLS, ALS, or SLS) with cross-platform observations capable of resolutions from  $10^{-3}$  m to  
206 continental scales (Figure 1). In terms of temporal extent, TLS, ALS and SLS are capable of  
207 employing weekly to sub-hourly repeat scan rates (Figure 1). Technologies allowing for faster

208 scan rates will typically limit the spatial extent (Figure 1). Advances in technology described in  
209 Section 2.3 will increase the spatial and temporal resolutions for all lidar platforms in the next  
210 five years (Figure 1). The intersecting process scales shown in Figure 1 demonstrate the viability  
211 of extracting transdisciplinary information from lidar given thoughtful experimental design and  
212 data collection.

213

## 214 **2.1 Lidar as a Transdisciplinary CZ Tool**

215 To investigate the state of the science of lidar in CZ research we conducted a literature review of  
216 147 peer-review papers that employed lidar datasets to improve process-based understanding.  
217 Our review found that most lidar studies to date have had a single disciplinary objective and that  
218 the CZ community is less likely to utilize the overlapping information in space and time  
219 generated by lidar (Figure 1). This is not surprising given the rampant progress made in filling  
220 important knowledge gaps in the individual cornerstone CZ disciplines using lidar datasets  
221 (Sections 1.1 to 1.3). We organized the literature reviewed for this paper into a scoring system of  
222 geomorphic, hydrologic, and ecologic process knowledge advanced through individual lidar-  
223 based studies. For each paper we assigned 10 points among the three disciplines to capture  
224 potential transdisciplinary lidar use. For example, a study leading purely to hydrologic process  
225 advances would rank as 10 in the hydrology category and zero in the ecology and  
226 geomorphology categories. A study balancing the process-based inferences among the three  
227 disciplines, with a more prominent ecological focus, would have been assigned scores of 3, 3,  
228 and 4 for geomorphology, hydrology, and ecology, respectively. Of course, this is a subjective  
229 scaling based on author opinions. To limit potential impacts of subjectivity, three different

230 authors of the current paper assigned independent scores to each study and we used the average  
231 score to place each paper in the relative ranking triangle (Figure 2).

232

233 The motivation for developing the conceptualization in Figure 2 is to facilitate identification of  
234 studies employing transdisciplinary synergies (e.g., lie within the internal triangle) that rely on  
235 the multi-faceted nature of lidar datasets. The review showed 38% of 147 studies were focused  
236 (score of 6 or higher) in geomorphology, 18% in hydrology, 32% in ecology, and the remainder  
237 had a more interdisciplinary focus. The few studies in the center of the triangle could be  
238 considered as potential exemplars of CZ science using lidar as they balance well among each  
239 cornerstone discipline. Several studies were transdisciplinary in nature, but focused on lidar-  
240 derived topography and did not maximize information content on hydrological and ecological  
241 processes from lidar: Pelletier et al. (2012), Persson et al. (2012), Brubaker et al. (2013), Pelletier  
242 (2013), Coops et al. (2013), Rengers et al. (2014), and Pelletier and Orem (2014). We instead  
243 draw focus to transdisciplinary studies that demonstrate the potential for complementary  
244 information to be extracted from lidar and integrated into field campaigns to allow multi-scale  
245 observations of interacting geomorphologic, hydrologic, and ecologic processes.

246

247 We highlight three studies that can serve as possible roadmaps to guide future transdisciplinary  
248 investigations using lidar datasets (Figure 2): Harman et al., 2014, Pelletier et al., 2013, and  
249 Perignon et al., 2013. These studies used complementary information from lidar to develop  
250 fundamental transdisciplinary advances in the theories and understanding of CZ processes and  
251 structure. For example, Harman et al. (2014) applied TLS to investigate coevolution of lidar-  
252 derived microtopography and vegetation (biovolume) at two 100-m long semi-arid hillslopes.

253 Integrating lidar and limited field measurements, Harman et al. (2014) found that both alluvial  
254 and colluvial processes were important in shaping vegetation and soil dynamics on hillslopes.  
255 The insights found by Harman et al. (2014) relied on the high resolution and precision of lidar  
256 information and would not have been possible using coarser traditional survey techniques for  
257 topography and vegetation structure. Pelletier et al. (2013) investigated landscape-scale (>10  
258 km<sup>2</sup>) variability in above-ground biomass, hydrologic routing, and topography derived from lidar  
259 at two mountain ranges in southern Arizona and applied a landscape evolution model to  
260 demonstrate the need to include ecological processes (e.g. vegetation density) to correctly model  
261 topography. Lidar-derived vegetation structure provided new information not attainable from  
262 other methods that allowed for Pelletier et al. (2013) to test a novel model of CZ development  
263 based on eco-pedo-geomorphic feedbacks. Perignon et al. (2013) investigated topographic  
264 change following a major flood along a 12 km stretch of the Rio Puerco in New Mexico. They  
265 found that sedimentation patterns reflected complex interactions of vegetation, hydraulics, and  
266 sediment at the scale of individual plants. This example demonstrates the value of lidar for  
267 testing ecohydrological resilience to extreme events and to develop new understanding of the  
268 fine-scale ecological feedbacks (i.e. individual plants) on reach scale geomorphic response.

269

270 These exemplar studies demonstrate the utility of lidar for transdisciplinary process  
271 investigations at scales ranging from hillslopes (e.g. Harman et al., 2014), to stream reaches (e.g.  
272 Perignon et al., 2013), to mountain ranges (e.g. Pelletier et al., 2013). We believe that these  
273 exemplar transdisciplinary studies should serve as motivation for increased use of lidar and  
274 integrated, multi-scale field observations for advancing CZ science. To this end, in Section 2.4

275 we provide additional examples to illustrate the overlapping processes observable with lidar that  
276 are motivated by CZ science questions.

277

## 278 **2.2 Applying Lidar in CZ Science**

279 Through our literature review and subsequent conceptualizations (e.g., Figure 1) we have  
280 identified three clear areas where lidar observations have the potential to advance the state of CZ  
281 science in the next five years: 1) quantifying change detection, 2) parameterization and  
282 verification of physical models, and 3) improving understanding of CZ processes across multiple  
283 scales. Applying these tools is not mutually exclusive and each area has different levels of  
284 previous research and development. For example, change detection utilizing lidar has received  
285 notable use in the CZ science community, particularly by geomorphologists analyzing  
286 topographic change over time. The use of lidar to quantify scaling relationships and thresholds  
287 remains relatively unexplored, despite robust scaling theories and analysis tools from other fields  
288 that are portable to lidar datasets. Similarly, integration of lidar datasets for either  
289 parameterization or verification has had limited development within CZ-relevant models.

290

### 291 **2.2.1 Change Detection**

292 Lidar-based change-detection analyses (CDA), i.e. mapping landscape adjustments through time  
293 in multi-temporal ALS and TLS datasets, have provided comprehensive measurements of snow  
294 depth (e.g. Harpold et al., 2014b; Tinkham et al., 2014) and ablation (Egli et al., 2012), co-  
295 seismic displacements after earthquakes (e.g. Oskin et al., 2012; Nissen et al., 2014), changes in  
296 aeolian dune form and migration rates (e.g. Pelletier, 2013), fluvial erosion (e.g. Anderson and  
297 Pitlick, 2014; Pelletier and Orem, 2014), earthflow displacements (e.g. DeLong et al., 2012),

298 knickpoint migration in gully/channel systems (e.g. Rengers and Tucker, 2014), cliff retreat  
299 along coasts (Young et al., 2010), permafrost degradation (Levy et al., 2013; Barnhart and  
300 Crosby, 2013), forest growth (Yu et al., 2004; Næsset and Gobakken, 2005), and changes in  
301 biomass (e.g. Meyer et al., 2013; Olsoy et al., 2014). Traditionally, lidar point clouds have been  
302 rasterized prior to differencing using open-source processing toolkits (e.g. GCD; e.g. Wheaton et  
303 al., 2010). However, new methods such as Iterative Closest Point (Nissen et al., 2012), particle  
304 image velocimetry (Aryal et al., 2012), and Multiscale Model to Model Cloud Comparison  
305 (Lague et al., 2013) enable direct differencing of point clouds. Continued methodological  
306 advances, coupled with increasingly available repeat datasets will progress the capabilities and  
307 quality of CDA. Structure from Motion (SfM) estimates three-dimensional structures from two-  
308 dimensional images providing an easily portable and low-cost method for making high-  
309 frequency change detection measurements (Westoby et al., 2012; Fonstad et al., 2013). There is  
310 also potential to apply time-series multi/hyperspectral lidar datasets to quantify changes in forest  
311 health over time. Similarly, integration of bathymetric lidar with ALS opens the potential to  
312 monitor dynamic changes in river flow and sediment transport (Flener et al., 2013). Although  
313 researchers often implement CDA using historic datasets (Rhoades et al., 2009), challenges arise  
314 from sparse metadata and reduced accuracy, thereby limiting dataset utility (e.g. Glennie et al.,  
315 2014). Future CDA may be improved by further establishing best practices for dataset sharing  
316 and archiving through repositories such as OpenTopography and UNAVCO.

317

### 318 **2.2.2 Scaling CZ Processes**

319 While researchers have harnessed existing scaling theories and tools utilizing lidar datasets, there  
320 is room for expansion using the range of scales afforded by lidar technologies (Figure 1). Two

321 complementary techniques, characterizing fractal patterns (e.g. Deems et al., 2006; Glenn et al.,  
322 2006; Perron et al., 2008) and process changes expressed as fractal breaks (e.g. Drake and  
323 Weishampel, 2000), benefit from the extensive breadth of spatial scales offered by lidar data.  
324 Self-similar patterns across scales indicate consistent processes and thus provide a framework for  
325 sampling, modeling, and re-scaling processes. Variograms and semi-variograms are commonly  
326 employed to plot lidar-derived attributes of interest such as snow distribution (e.g. Deems et al.,  
327 2008; Harpold et al., 2014a) or forest spatial patterns (e.g. Boutet et al., 2003) against scale.  
328 Fractal and fractal deviations, as well as the length-scales of landscape structure (Perron et. al.,  
329 2008), convey important CZ information, e.g., the effect of tree-root spacing through time on soil  
330 production (Roering et al., 2010), patterns in tree gap-formation (Plotnick et al., 1996; Frazer et  
331 al., 2005), and underlying abiotic and biotic controls on forest fractal dimensions (Drake and  
332 Weishampel, 2000). Within the CZ framework, lidar allows consideration of topographic  
333 variation and biomass distribution (Chorover et al., 2011), and spatial thresholds for interactions  
334 among vegetation, hydrology, lithology, and surface processes ranging from the grain to  
335 landscape scale (e.g., Musselman et al., 2013; Pelletier et al., 2013; Harman et al., 2014). Zhao et  
336 al. (2009) developed a scale-invariant model of forest biomass, which illustrated the utility of  
337 scale-independent methods. However, we caution that one scientist's signal may be another's  
338 noise (Tarolli, 2014). Signal recognition may involve smoothing at one scale to quantify a  
339 relevant landscape metric, such as hillslope curvature (and derived erosion rates) (Hurst et al.,  
340 2013), which in turn limits valuable information at another scale, such as hydrologically-driven  
341 surface roughness or the spacing of tree-driven bedrock disruption (Roering et al., 2010; Hurst et  
342 al., 2012). Overall, lidar datasets retain the promise of up- or down- scaling feedbacks among  
343 multiple processes that are just beginning to be fully utilized.

344

### 345 ***2.2.3 Model Parameterization and Verification***

346 The wealth of recently collected lidar data has potential to inform the choice of physically-based  
347 model parameters and verify model output. Improved terrain representation has helped  
348 characterize hysteretic relationships between water storage and contributing area in large wetland  
349 complexes within parameterized runoff models (Shook et al., 2013), improved mapping in and  
350 along river channels to parameterize network level structure and flood inundation models  
351 (French, 2003; Kinzel et al., 2007; Snyder, 2009; Bates, 2012), and expanded investigation of  
352 geomorphological change in floodplains (Thoma et al., 2005; Jones et al., 2007). Lidar provides  
353 vertical information that permits the direct retrieval of forest attributes such as tree height and  
354 canopy structure (Hyypä et al., 2012; Vosselman and Maas, 2010) that can be used to model  
355 canopy volume (Palminteri et al., 2012), biomass (Zhao et al., 2009), and the transmittance of  
356 solar radiation (Essery et al., 2008; Musselman et al., 2013; Bode et al., 2014). Lidar has also  
357 proven to be instrumental in the verification of model states. For example, lidar datasets have  
358 been used to verify physically-based models, including landscape evolution models (Pelletier et  
359 al., 2014; Pelletier and Perron, 2012; Rengers and Tucker, 2014), aeolian models (Pelletier et al.,  
360 2012; Pelletier, 2013), physiological models (Coops et al., 2013), snowpack energy balance  
361 models (Essery et al., 2008, Broxton et al., 2015), and an ecosystem dynamics model  
362 (Antonarakis et al., 2014). Simpler, empirical models have also been developed using lidar-  
363 derived estimates of soil erosion (Pelletier and Orem, 2014) and snow accumulation and ablation  
364 (Varhola et al., 2014). Better recognition of the potential benefits of lidar for model calibration  
365 and verification within CZ modeling communities could lead to increased utilization and targeted  
366 acquisitions in the future.

367

## 368 **2.3 Adoption and Utilization of Lidar Datasets**

369 New and improved lidar datasets are more likely to result in transformative CZ science if a  
370 number of key opportunities (and impediments) are recognized. The research topics discussed in  
371 Section 2.2 require attention to four key areas in order to maximize the applicability of lidar in  
372 CZ science: 1) Emerging data acquisition technologies, 2) Availability of processing and  
373 analysis techniques, 3) Linkages to *in situ* observations, and 4) Linkages to other remote sensing  
374 observations. The first two areas recognize the importance of technological advances and  
375 information sharing to enhance lidar data quality and coverage. The second two areas  
376 demonstrate the potential to extend scientific inferences made from lidar with linkages to  
377 multiple, complementary observations.

378

### 379 **2.3.1 Data Acquisition Technology**

380 Future advances in data acquisition technologies will provide greater information and  
381 spatiotemporal coverage from lidar (and similar high-resolution remote sensing technologies)  
382 datasets. Several new lidar technologies are rapidly increasing data quality (accuracy, precision,  
383 resolution, etc.) and information content. Full waveform lidar data promises to provide better  
384 definition of ground surface and vegetation canopy (Wagner et al., 2008, Mallet and Bretar,  
385 2009). Utilizing blue-green light spectrum, lidar systems are capable of bathymetric profiling  
386 (McKean et al., 2009; Fernandez-Diaz et al., 2014) and potentially determining turbidity and  
387 inherent optical properties of the water column. Lidar systems have demonstrated the benefits of  
388 combining point clouds with alternative data sources by, for example, including intensity and/or  
389 RGB cameras (Bork and Su, 2007) that collect data synchronously with the lidar and provide

390 metadata for each point in the cloud. Less expensive and more adaptable lidar systems (Brooks et  
391 al., 2013) and alternative 3-D remote sensing techniques, such as SfM or low-cost 3D cameras  
392 (Mankoff and Russo, 2013; Javernick et al., 2014; Lam et al., 2015), promise high resolution  
393 monitoring at finer temporal resolutions and lower costs. Increasingly, lidar observations are  
394 combined with passive electro-optical multispectral and hyperspectral images (Kurz et al., 2011).  
395 Lidar technology already includes active multispectral laser systems, and hyperspectral laser  
396 observations of object reflectance are likely only three to five years away (Hakala et al., 2012;  
397 Hartzell et al., 2014). These systems promise to lessen the need for multiple sensors, thus  
398 reducing uncertainties due to data registration, lowering costs, and reducing processing time. The  
399 combination of these technologies holds promise as a means to cost-effectively monitor aspects  
400 of the CZ at time scales of days or less and information content that includes not only 3D  
401 structure, but also spectral information that is potentially capable of determining vegetation  
402 composition and health, soil and exposed bedrock composition, and soil water content.

403

404 In addition to emerging lidar acquisition systems, new and existing collection platforms are  
405 substantially broadening data coverage. Collection of lidar from fixed-wing aircraft is expanding  
406 to national scales through programs such as the U.S. Geological Survey's 3-D Elevation Program  
407 (3DEP), Switzerland's national lidar dataset collected by the Federal Office of Topography,  
408 Sweden's Lantmäteriet (<http://www.lantmateriet.se>), Netherlands' Public Map Service  
409 (<http://www.pdok.nl/en/node>), Denmark's Geodata Agency (<http://gst.dk>), Finland's National  
410 Land Survey (<http://www.maanmittauslaitos.fi/en/maps-5>), United Kingdom's Environment  
411 Agency (<http://www.geomatics-group.co.uk/GeoCMS>), and Australia's AusCover  
412 (<http://www.auscover.org.au/>). Additionally, acquisition of aircraft and lidar systems by

413 institutional research programs have led to greater capabilities for ecological research by the  
414 National Ecological Observatory Network (Kampe et al., 2010) and snow water resources via  
415 NASA's Airborne Snow Observatory (<http://aso.jpl.nasa.gov>). Institutional systems and  
416 operational expertise are also available for short-term research projects across a range of Earth  
417 science applications (Glennie et al., 2013) via the National Center for Airborne Laser Mapping  
418 (NCALM) and UNAVCO. Of particular interest to the CZ community is the development of  
419 unmanned aerial systems (UASs) that are capable of mounting small lidar systems for rapid  
420 deployment (Lin et al., 2011; Wallace et al., 2012). Long-range UASs offer the potential for  
421 repeat lidar acquisitions at a fraction of the cost of current ALS platforms. Best practices for  
422 collecting, processing and analyzing lidar over increasing extents (i.e. continental scales) are  
423 generally lacking, which can limit the effectiveness of datasets collected over vastly different  
424 physiographic conditions.

425

### 426 ***2.3.2 Data Access, Processing, and Analysis***

427 The crux of successfully leveraging a flood of new lidar (and other high-resolution topographic  
428 information) data for CZ science (e.g. Stennett, 2004) will be the ability to extract meaningful  
429 information from these rich and voluminous datasets. These new lidar datasets require data  
430 processing and analysis tools be optimized to handle increasingly large datasets with greater  
431 information content. Processing limitations are likely to reduce the usability and extent of very  
432 high information datasets, e.g. waveform or multispectral datasets pose processing challenges at  
433 the continental scale but may be more manageable at the watershed scale. Further, new software  
434 and workflows need to be developed that enable scientists to incorporate lidar data into detailed  
435 models of the CZ without expertise in remote sensing. The CZ science community must engage

436 in a concerted effort to develop (and/or adopt from other domains) new open source tools that  
437 leverage high performance computing resources available through programs such as NSF's  
438 XSEDE (<https://www.xsede.org/home>). By increasing the scalability of CZ lidar-oriented  
439 processing and analysis tools, computationally intensive analysis and modeling at the highest  
440 resolution of the lidar datasets will be possible. In addition to increasing software scalability,  
441 new processing tools are necessary to take advantage of new data types, such as full waveform  
442 lidar (Wagner et al., 2008, Mallet and Bretar, 2009) and hyperspectral laser technology (Hakala  
443 et al., 2012). Cloud computing and the "big data paradigm" that is increasingly common in both  
444 industry and academia (Mattman, 2013) present opportunities for the CZ lidar community. One  
445 such opportunity for big data sharing is EarthCube (<http://www.earthcube.org>), a relatively new  
446 program that has potential to integrate lidar information (among other geospatial information)  
447 into data sharing efforts in the geosciences. Due to efforts such as NSF's OpenTopography  
448 (Crosby et al., 2011), there is a large volume of CZ-oriented lidar online and freely available to  
449 the community. For example, OpenTopography already offers on-demand processing services  
450 (Krishnan et al., 2011) that permit users to generate standard and commonly used derivatives  
451 from the hosted lidar point cloud. By coupling data processing with data access, users are not  
452 required to download large volumes of data locally or have the dedicated computing and  
453 software resources to process these data. Although many CZ-oriented lidar datasets are already  
454 available to the community through resources such as OpenTopography in the U.S., there are  
455 numerous other lidar datasets globally that are not accessible because they are not available  
456 online or access is restricted. Many of these "legacy" datasets are likely to be important temporal  
457 baselines for comparison against future datasets (Glennie et al., 2014; Harpold et al., 2014a).  
458

### 459 2.3.3 Linkages To In Situ Observations

460 Many CZ studies have incorporated *in situ* observations to extend or confirm inferences made  
461 with lidar-derived datasets. *In situ* measurements are time consuming to collect, often expensive  
462 to analyze, and limited in terms of spatial coverage. As a result, researchers must be judicious  
463 with *in situ* data collection and maximize integration with lidar datasets. Physical and chemical  
464 properties of soil and rock, and vegetation structure are among the *in situ* observations  
465 commonly integrated with lidar datasets. For example, lidar-based studies have integrated  
466 distributed measurements of soil hydraulic properties (Harman et al., 2014) and soil thickness  
467 (Roering et al., 2010; Pelletier et al., 2014; West et al., 2014), as well as radioactive isotopes in  
468 soils (West et al., 2014). Lidar datasets have also been used to extend *in situ* observations of  
469 snow depth (Harpold et al., 2014a; Varhola and Coops, 2013) and carbon fluxes (Hudak et al.,  
470 2012) in both space and time. *In situ* observations of vegetation structural characteristics are  
471 commonly made to develop relationships with lidar observations and extend these relationships  
472 for forest inventory (e.g. Wulder et al., 2002). In addition to scientific inferences, lidar can be  
473 used to improve sampling design to reduce field time and analytical expenses. For example, lidar  
474 has improved insight into sampling snow measurements necessary for water management  
475 (McCreight et al., 2014). A number of challenges remain to link lidar-derived information to *in*  
476 *situ* measurements, including poor GPS information for historical datasets, constraining the  
477 observational footprint of different measurements, and comparing lidar-derived metrics to typical  
478 field measurements. Despite these challenges, opportunities exist to better integrate historical  
479 measurements into lidar-based studies and develop new *in situ* observations that use lidar  
480 datasets to up-scale CZ processes.

481

#### 482 **2.3.4 Linkages to Satellite Remote Sensing**

483 Satellite observations of surface-altimetry, reflectance, permittivity, and atmospheric profiles  
484 provide observations of CZ processes at multiple spatiotemporal scales, frequently with global  
485 coverage. The high spatial resolution offered by lidar technology complements the regular  
486 temporal frequency of optical and radar satellite observations, which could be used to co-  
487 calibrate and co-validate these types of datasets. Satellites also provide another platform for lidar  
488 acquisition. There are numerous examples where lidar datasets have been used to calibrate and  
489 verify coarser estimates of vegetation, cryosphere (e.g. glaciers, permafrost, snowpacks, etc.),  
490 and geomorphic processes and states made via optical and radar satellites. For example, Mora et  
491 al. (2013) used detailed lidar measurements of vegetation structure to quantify the spatial and  
492 temporal scalability of above ground biomass of continental forests measured with the very high  
493 spatial resolution (VHSR) satellite. In data-limited regions of Uganda, lidar fused with Landsat  
494 datasets have improved modeled biomass predictions and understanding of phenologic processes  
495 (Avitable et al., 2012). Varhola and Coops (2013) and Ahmed et al. (2014) introduce methods  
496 for detecting changes in vegetation structure and function from disturbance by fusing Landsat  
497 and lidar measurements, and Bright et al. (2014) used similar fused datasets to investigate  
498 changes following forest mortality. Applications combining lidar and satellite measurements to  
499 change detection have also been applied to evaluate the effects of vegetation on snowpack  
500 dynamics (Varhola et al., 2014) and for comparison with model and satellite-derived estimates of  
501 snow-covered area (Kirchner et al., 2014; Hedrick et al., 2014). A multifaceted approach for the  
502 prediction and monitoring of landslides by Guzzetti (2012) used measurements from optical  
503 satellites and lidar. The Ice, Cloud, and land Elevation Satellite (ICESat) was a NASA mission  
504 from 2003 to 2009 that mapped changes in glacier mass balance using SLS (Kohler et. al. 2013).

505 Scientists have used ICESat's Geoscience Laser Altimeter System (GLAS) to identify areas of  
506 forest regeneration along the Mississippi (Li et al., 2011) and it has been applied in development  
507 of a global forest height map (Simard et al., 2011). A second mission (ICESat-2) is slated to  
508 launch in 2017 and while focused on ice sheet and sea ice change, it will provide complementary  
509 products to characterize terrestrial ecology. Furthermore, other current and future satellite  
510 missions will provide CZ observations that integrate with lidar, including soil moisture,  
511 groundwater storage, soil freeze/thaw, carbon flux, and primary productivity (Schimel et. al.,  
512 2013). Of particular interest might be the Surface Water and Ocean Topography (SWOT)  
513 mission that provides coarse water and land topography using radar that has potential to  
514 complement finer-scale measurements acquired with lidar. To fully realize the potential  
515 information available from fused lidar and satellite datasets, critical attention must be paid to 1)  
516 efficient processing of large datasets that span collection platforms and spatiotemporal  
517 variability, and 2) maintaining expert knowledge in data interpretation (Mattmann, 2013).

518

#### 519 **2.4 A Proposed Five-Year Vision**

520 The fields of CZ science and lidar-based technology are both advancing rapidly. Here, we  
521 present a vision that keeps CZ researchers abreast of advances in lidar technologies and positions  
522 CZ science at the forefront of the lidar revolution, particularly with regards to new hardware,  
523 processing capabilities, and linkages with complementary observations. These ideas are guided  
524 by the recognition that lidar is capable of simultaneously observing process signatures from  
525 multiple CZ disciplines (Figure 1). To elucidate this point, we discuss three examples of  
526 transdisciplinary CZ research questions and suggest how they could benefit from current and  
527 future lidar technologies. We also provide specific recommendations for CZ researchers working

528 with (or considering working with) with lidar datasets. Our intent is to catalyze CZ interest in the  
529 transdisciplinary possibilities of lidar datasets, while increasing the influence of CZ scientists  
530 within the broader group of lidar end-users.

531

532 Technological advances can be conceptualized as increasing data coverage, quality, and  
533 information, including new acquisition platforms or higher acquisition rates (Figure 3). Other  
534 advances, such as full-waveform information or hyperspectral lasers, will increase the data  
535 quality and information content extractable from lidar datasets. Three examples of linked  
536 transdisciplinary research questions (Figure 3) demonstrate the value of technological advances  
537 in lidar for CZ science: 1) How does co-variation between vegetation and hydrological flowpaths  
538 control the likelihood and distribution of earth flows and landslides?, 2) How is the rapidly  
539 changing cryosphere influencing hydrological connectivity, drainage network organization,  
540 nutrient and sediment fluxes, land-surface energy inputs, and vegetation structure?, 3) How does  
541 above- and below-ground biomass control bedrock to soil production rates, sediment mixing and  
542 transport, and associated carbon fluxes via bioturbation and hillslope transport? These example  
543 questions demonstrate the need for research that transcends information sharing across  
544 disciplines to develop synergistic new theories and advances in CZ science.

545

546 These research questions span a wide-range of spatial and temporal scales, from smaller and  
547 faster ( $10^{-2}$  m and  $10^1$  s) in Question 3 to larger and more long-term ( $10^5$  m and  $10^6$  s) in  
548 Question 2 (see Figure 1). Our ability to answer these questions benefits from several facets of  
549 improved lidar technologies, including higher acquisition rates and larger ranges, more rapid and  
550 robust deployment options, and improved processing resources for extracting information. Future

551 lidar technologies could address Question 1 by identifying specific vegetation species via  
552 hyperspectral laser technologies, increasing accuracy of bare-earth estimation to improve  
553 hydrologic routing using full waveform analysis, and increasing coverage of landslide-prone  
554 areas from different physiographic regions (Figure 3). New technology will address Question 2  
555 by providing estimates of riparian vegetation productivity, measuring channel bathymetry using  
556 blue-green lidar, and with new platforms that increase sampling frequency via UASs or other  
557 low cost systems. Lastly, new technology will address Question 3 by providing improved  
558 estimates of above-ground biomass and bare-earth extraction using full waveform analysis, and  
559 improved fine-scale change detection with greater processing resources. These example  
560 questions and their conceptualization (Figure 3) demonstrate what well-integrated lidar datasets  
561 can provide to stimulate and improve future CZ research.

562

563 We propose five recommendations as an attempt to unite the CZ community around improved  
564 utilization and advocacy of lidar technology in important transdisciplinary scientific contexts that  
565 integrate the opportunities and impediments discussed previously:

566 · **Open lines of communication:** Develop communication within and among groups,  
567 including individual CZ disciplines, remote sensing scientists, computer scientists, private  
568 industry, and funding agencies. Workshops have the potential to increase communication  
569 between “data users” and “data creators”. CZ scientists must find ways to communicate their  
570 data acquisition specifications to the scientists and engineers who create lidar hardware and  
571 processing software through venues such as meetings with private industry, the development of  
572 advisory committees, and commentary pieces in trade journals that present a vision for the future  
573 needs of CZ scientists. Open communication among diverse CZ scientists is fundamental to

574 developing collaborations capable of transdisciplinary advances. Working groups within CZ  
575 communities, like the critical zone exploration network (<http://www.czen.org>), and townhall  
576 meetings at international Earth science conferences have initiated sustainable communication  
577 venues. Future efforts focused on early-career CZ scientists that demonstrate the benefits of  
578 transdisciplinary efforts, such as focused conferences and pilot research projects, should be  
579 pursued.

580 ·       **Increase information extraction:** Advocate for lidar repositories that are interoperable  
581 and broaden data access, as well as open-source and community-centric processing resources.  
582 Ultimately, enhanced and streamlined data processing and analysis tools will enable CZ  
583 researchers to concentrate on understanding fundamental science problems instead of struggling  
584 with data access, processing, and analysis. Specifically, recent efforts focused on cloud storage  
585 and computing resources, and open source software tools could greatly aid this effort. Efforts to  
586 improve the efficiency of processing will become more important as the acquisition of lidar  
587 expands to continental scales. Information extraction at larger extents will require judicious  
588 tradeoffs between acquisition parameters and costs that consider variability in local  
589 physiographic conditions (i.e. higher sampling densities in areas with dense vegetation cover and  
590 high topographic complexity). Programs to support open source software and their long-term  
591 sustainability are required to support CZ science. Increasing open access to lidar datasets  
592 facilitates greater information extraction and the potential for meta-analysis studies. The value of  
593 open-access datasets will increase as improved processing tools become available. CZ scientists  
594 should also consider working with private lidar acquisition companies and their customers (i.e.  
595 forestry, mining, and urban planning organizations) to release what has previously been  
596 proprietary data to the public.

597 ·       **Increase accessibility of lidar systems:** Advocate for new acquisition technologies that  
598 lower the cost of lidar collection and increase its availability, such as unmanned platforms and  
599 less expensive and longer-range lidar systems. Institutional acquisitions of lidar systems also  
600 significantly increase accessibility. Community-supported lidar systems available to researchers,  
601 through agencies, such as UNAVCO and NCALM, should also be encouraged. A powerful  
602 advancement would be a “clearinghouse” where agencies and institutions could exchange  
603 information on lidar systems, seek expert advice on lidar acquisition, and potentially trade or rent  
604 hardware to better meet the needs of individual projects.

605 ·       **Focus on key technologies:** Support the development of new lidar technologies that are  
606 useful for linking disciplinary observations. For example, our review has stressed the potential  
607 benefits for linking CZ functions to processes offered by hyperspectral laser technologies (Figure  
608 3). Other key technologies include new acquisition platforms (UASs) and improved open-source  
609 processing capabilities and open-source industry-standard data formats. The community should  
610 continue a dialogue about critical technologies within CZ science venues in parallel with  
611 interactions with technology developers (as mentioned previously). The more united the CZ  
612 community is about the benefits of a particular technology (i.e. hyperspectral lidar) the more it  
613 can advocate within public and private sectors for its advancement.

614 ·       **Link complementary observations:** Consider other remote sensing observations that  
615 may be complementary to lidar (e.g. thermal, infrared, optical, and microwave). While fusing  
616 remote sensing data is becoming more common, the value of lidar information to coarser remote  
617 sensing products is vast and underutilized. Be mindful of the potential synergistic benefits of  
618 collecting lidar data over areas with *in situ* observations and vice versa, consider how to improve  
619 collection of *in situ* observations based on lidar information. In particular, *in situ* information

620 collected during lidar data collection can be extremely valuable and difficult to substitute for at a  
621 later date. Maintain awareness of competing, less expensive technologies, such as SfM, that may  
622 be more appropriate in some conditions and geographical locations. The multi-scale nature of  
623 transdisciplinary research (Figures 1 and 3) demands that lidar be integrated into a broader  
624 observational framework that does not neglect the value of *in situ* and coarser remote sensing  
625 observations.

626

627 **Acknowledgements:**

628 The workshop forming the impetus for this paper was funded by the National Science  
629 Foundation (EAR 1406031). Additional funding for the workshop and planning was provided to  
630 S.W. Lyon by the Swedish Foundation for International Cooperation in Research and Higher  
631 Education (STINT Grant No. 2013-5261). A.A. Harpold was supported by an NSF fellowship  
632 (EAR 1144894). The use of specific commercial or open-source packages and tools in this paper  
633 does not imply a specific endorsement.

634

635

636 **References:**

- 637 Abdalati, W., H.J. Zwally, R. Bindenschadler, B. Csatho, S.L. Farrell, H.A. Fricker, D. Harding, R.  
638 Kwok, M. Lefsky, T. Markus, A. Marshak, T. Neumann, S. Palm, B. Schutz, B. Smith, J.  
639 Spinhirne, and C. Webb (2010), The ICESat-2 laser altimetry mission. *Proceedings of the*  
640 *IEEE*, 98(5), 735-751, doi: 10.1109/JPROC.2009.2034765
- 641 Ahmed, O. S., S. E. Franklin, and M. A. Wulder (2014), Interpretation of forest disturbance  
642 using a time series of Landsat imagery and canopy structure from airborne LiDAR,  
643 *Canadian Journal of Remote Sensing*, 39(6), 521–542, doi:10.5589/m14-004.
- 644 Anderson, S., and J. Pitlick (2014), Using repeat LiDAR to estimate sediment transport in a steep  
645 stream, *J. Geophys. Res. Earth Surf.*, 119(3), 621–643, doi:10.1002/2013JF002933.
- 646 Antonarakis, A. S., J. W. Munger, and P. R. Moorcroft (2014), Imaging spectroscopy- and  
647 LiDAR-derived estimates of canopy composition and structure to improve predictions of  
648 forest carbon fluxes and ecosystem dynamics, *Geophysical Research Letters*, 41(7),  
649 2013GL058373, doi:10.1002/2013GL058373.
- 650 Antonarakis, A. S., K. S. Richards, J. Brasington, and E. Muller (2010), Determining leaf area  
651 index and leafy tree roughness using terrestrial laser scanning, *Water Resources Research*,  
652 46(6), W06510, doi:10.1029/2009WR008318.
- 653 Arnold, N. S., W. G. Rees, B. J. Devereux, and G. S. Amable (2006), Evaluating the potential of  
654 high-resolution airborne LiDAR data in glaciology, *International Journal of Remote*  
655 *Sensing*, 27(6), 1233–1251, doi:10.1080/01431160500353817.
- 656 Aryal, A., B. A. Brooks, M. E. Reid, G. W. Bawden, and G. R. Pawlak (2012), Displacement  
657 fields from point cloud data: Application of particle imaging velocimetry to landslide  
658 geodesy, *Journal of Geophysical Research: Atmospheres (1984–2012)*, 117(F1), F01029,  
659 doi:10.1029/2011JF002161.
- 660 Asner, G. P., D. E. Knapp, J. Boardman, R. O. Green, T. Kennedy-Bowdoin, M. Eastwood, R. E.  
661 Martin, C. Anderson, and C. B. Field (2012a), Carnegie Airborne Observatory-2: Increasing  
662 science data dimensionality via high-fidelity multi-sensor fusion, *Remote Sensing of*  
663 *Environment*, 124(0), 454–465, doi:10.1016/j.rse.2012.06.012.
- 664 Asner, G., J. Mascaro, H. Muller-Landau, G. Vieilledent, R. Vaudry, M. Rasamoelina, J. Hall,  
665 and M. van Breugel (2012b), A universal airborne LiDAR approach for tropical forest  
666 carbon mapping, *Oecologia*, 168(4), 1147–1160, doi:10.1007/s00442-011-2165-z.

667 Avitabile, V., A. Baccini, M. A. Friedl, and C. Schmullius (2012), Capabilities and limitations of  
668 Landsat and land cover data for aboveground woody biomass estimation of Uganda, *Remote*  
669 *Sensing of Environment*, 117(0), 366–380, doi:10.1016/j.rse.2011.10.012.

670 Baccini, A. et al. (2012), Estimated carbon dioxide emissions from tropical deforestation  
671 improved by carbon-density maps, *Nature Climate change*, 2(3), 182–185,  
672 doi:10.1038/nclimate1354.

673 Barnhart, T. B., and B. T. Crosby (2013), Comparing Two Methods of Surface Change Detection  
674 on an Evolving Thermokarst Using High-Temporal-Frequency Terrestrial Laser Scanning,  
675 Selawik River, Alaska, *Remote Sensing*, 5(6), 2813–2837, doi:10.3390/rs5062813.

676 Bates, P. D. (2012), Integrating remote sensing data with flood inundation models: how far have  
677 we got? *Hydrol. Process.*, 26(16), 2515–2521, doi:10.1002/hyp.9374.

678 Belmont, P. et al. (2011), Large Shift in Source of Fine Sediment in the Upper Mississippi River,  
679 *Environ. Sci. Technol.*, 45(20), 8804–8810, doi:10.1021/es2019109.

680 Bittner, S., S. Gayler, C. Biernath, J. B. Winkler, S. Seifert, H. Pretzsch, and E. Priesack (2014),  
681 Evaluation of a ray-tracing canopy light model based on terrestrial laser scans, *Canadian*  
682 *Journal of Remote Sensing*, 38(5), 619–628, doi:10.5589/m12-050.

683 Bode, C. A., M. P. Limm, M. E. Power, and J. C. Finlay (2014), Subcanopy Solar Radiation  
684 model: Predicting solar radiation across a heavily vegetated landscape using LiDAR and GIS  
685 solar radiation models, *Remote Sensing of Environment*, (0 SP - EP - PY - T2 -),  
686 doi:10.1016/j.rse.2014.01.028.

687 Booth, A. M., J. J. Roering, and J. T. Perron (2009), Automated landslide mapping using spectral  
688 analysis and high-resolution topographic data: Puget Sound lowlands, Washington, and  
689 Portland Hills, Oregon, *Geomorphology*, 109(3-4), 132–147,  
690 doi:10.1016/j.geomorph.2009.02.027.

691 Bork, E. W., and J. G. Su (2007), Integrating LIDAR data and multispectral imagery for  
692 enhanced classification of rangeland vegetation: A meta analysis, *Remote Sensing of*  
693 *Environment*, 111(1), 11–24, doi:10.1016/j.rse.2007.03.011.

694 Boutet, J., Jr, and J. Weishampel (2003), Spatial pattern analysis of pre- and post-hurricane forest  
695 canopy structure in North Carolina, USA, *Landscape Ecology*, 18(6), 553–559,  
696 doi:10.1023/A%3A1026058312853.

697 Brasington, J., D. Vericat, and I. Rychkov (2012), Modeling river bed morphology, roughness,

698 and surface sedimentology using high resolution terrestrial laser scanning, *Water Resources*  
699 *Research*, 48(11), W11519, doi:10.1029/2012WR012223.

700 Bright, B. C., A. T. Hudak, R. McGaughey, H.-E. Andersen, and J. Negrón (2014), Predicting  
701 live and dead tree basal area of bark beetle affected forests from discrete-return LiDAR,  
702 *Canadian Journal of Remote Sensing*, 39(sup1), S99–S111, doi:10.5589/m13-027.

703 Brooks, B. A., C. Glennie, K. W. Hudnut, T. Ericksen, and D. Hauser (2013), Mobile Laser  
704 Scanning Applied to the Earth Sciences, *Eos, Transactions American Geophysical Union*,  
705 94(36), 313–315, doi:10.1002/2013EO360002.

706 Broxton, P. D., A. A. Harpold, P. D. Brooks, P. A. Troch, and N. P. Molotch (In Press),  
707 Quantifying the effects of vegetation structure on wintertime vapor losses from snow in  
708 mixed-conifer forests, *Ecohydrol*.

709 Brubaker, K. M., W. L. Myers, P. J. Drohan, D. A. Miller, and E. W. Boyer (2013), The Use of  
710 LiDAR Terrain Data in Characterizing Surface Roughness and Microtopography, *Applied*  
711 *and Environmental Soil Science*, 2013, 13, doi:10.1155/2013/891534.

712 Cho, M. A. et al. (2012), Mapping tree species composition in South African savannas using an  
713 integrated airborne spectral and LiDAR system, *Remote Sensing of Environment*, 125(0),  
714 214–226, doi:10.1016/j.rse.2012.07.010.

715 Chorover, J. et al. (2011), How Water, Carbon, and Energy Drive Critical Zone Evolution: The  
716 Jemez–Santa Catalina Critical Zone Observatory, *Vadose Zone Journal*, 10(3), 884–899.

717 Coops, N. C., F. Morsdorf, M. E. Schaepman, and N. E. Zimmermann (2013), Characterization  
718 of an alpine tree line using airborne LiDAR data and physiological modeling, *Global*  
719 *Change Biology*, 19(12), 3808–3821, doi:10.1111/gcb.12319.

720 Crosby, C., R. Arrowsmith, V. Nandigam, and C. Baru (2011), Online access and processing of  
721 LiDAR topography data, edited by G. R. Keller and C. Baru, Cambridge University Press.

722 Day, S. S., K. B. Gran, P. Belmont, and T. Wawrzyniec (2013), Measuring bluff erosion part 1:  
723 terrestrial laser scanning methods for change detection, *Earth Surface Processes and*  
724 *Landforms*, 38(10), 1055–1067, doi:10.1002/esp.3353.

725 Deems, J. S., S. R. Fassnacht, and K. J. Elder (2006), Fractal Distribution of Snow Depth from  
726 LiDAR Data, *J. Hydrometeor*, 7(2), 285–297, doi:10.1175/JHM487.1.

727 Deems, J. S., S. R. Fassnacht, and K. J. Elder (2008), Interannual Consistency in Fractal Snow  
728 Depth Patterns at Two Colorado Mountain Sites, *J. Hydrometeor*, 9(5), 977–988,

729 doi:10.1175/2008JHM901.1.

730 Deems, J. S., T. H. Painter, and D.C. Finnegan (2013), LiDAR measurement of snow depth: a  
731 review, *Journal of Glaciology*, 59(215), 467-479, doi.org/10.3189/2013JoG12J154

732 DeLong, S. B., C. S. Prentice, G. E. Hilley, and Y. Ebert (2012), Multitemporal ALSM change  
733 detection, sediment delivery, and process mapping at an active earthflow, *Earth Surface  
734 Processes and Landforms*, 37(3), 262–272, doi:10.1002/esp.2234.

735 Dickinson, Y., E. K. Zenner, and D. Miller (2014), Examining the effect of diverse management  
736 strategies on landscape scale patterns of forest structure in Pennsylvania using novel remote  
737 sensing techniques, *Can. J. For. Res.*, 44(4), 301–312, doi:10.1139/cjfr-2013-0315.

738 Drake, J. B., and J. F. Weishampel (2000), Multifractal analysis of canopy height measures in a  
739 longleaf pine savanna, *Forest Ecology and Management*, 128(1–2), 121–127,  
740 doi:10.1016/S0378-1127(99)00279-0.

741 Egli, L., T. Jonas, T. Grünewald, M. Schirmer, and P. Burlando (2012), Dynamics of snow  
742 ablation in a small Alpine catchment observed by repeated terrestrial laser scans, *Hydrol.  
743 Process.*, 26(10), 1574–1585, doi:10.1002/hyp.8244.

744 Essery, R., P. Bunting, A. Rowlands, N. Rutter, J. Hardy, R. Melloh, T. Link, D. Marks, and J.  
745 Pomeroy (2008), Radiative Transfer Modeling of a Coniferous Canopy Characterized by  
746 Airborne Remote Sensing, *J. Hydrometeor*, 9(2), 228–241, doi:10.1175/2007JHM870.1.

747 Fassnacht, S. R., and J. S. Deems (2006), Measurement sampling and scaling for deep montane  
748 snow depth data, *Hydrol. Process.*, 20(4), 829–838, doi:10.1002/hyp.6119.

749 Fernandez-Diaz, J. C., C. L. Glennie, W. E. Carter, R. L. Shrestha, M. P. Sartori, A. Singhanian,  
750 C. J. Legleiter, and B. T. Overstreet (2014), Early Results of Simultaneous Terrain and  
751 Shallow Water Bathymetry Mapping Using a Single-Wavelength Airborne LiDAR Sensor,  
752 *Selected Topics in Applied Earth Observations and Remote Sensing, IEEE Journal of*, 7(2),  
753 623–635, doi:10.1109/JSTARS.2013.2265255.

754 Fewtrell, T. J., P. D. Bates, M. Horritt, and N. M. Hunter (2008), Evaluating the effect of scale in  
755 flood inundation modelling in urban environments, *Hydrol. Process.*, 22(26), 5107–5118,  
756 doi:10.1002/hyp.7148.

757 Féret, J.-B., and G. P. Asner (2012), Semi-Supervised Methods to Identify Individual Crowns of  
758 Lowland Tropical Canopy Species Using Imaging Spectroscopy and LiDAR, *Remote  
759 Sensing*, 4(8), 2457–2476, doi:10.3390/rs4082457.

760 Flener, C., M. Vaaja, A. Jaakkola, A. Krooks, H. Kaartinen, A. Kukko, E. Kasvi, H. Hyypä, J.  
761 Hyypä, and P. Alho (2013), Seamless Mapping of River Channels at High Resolution  
762 Using Mobile LiDAR and UAV-Photography, *Remote Sensing*, 5(12), 6382–6407,  
763 doi:10.3390/rs5126382.

764 Fonstad, M. A., J.T. Dietrich, B.C. Courville, J.L Jensen, and P.E. Carbonneau (2013).  
765 Topographic structure from motion: a new development in photogrammetric measurement,  
766 *Earth Surface Processes and Landforms*, 38(4), 421-430, doi: 10.1002/esp.3366.

767 Forzieri, G., G. Moser, E. R. Vivoni, F. Castelli, and F. Canovaro (2010), Riparian Vegetation  
768 Mapping for Hydraulic Roughness Estimation Using Very High Resolution Remote Sensing  
769 Data Fusion, *Journal of Hydraulic Engineering*, 136(11), 855–867,  
770 doi:10.1061/(ASCE)HY.1943-7900.0000254.

771 Frazer, G. W., M. A. Wulder, and K. O. Niemann (2005), Simulation and quantification of the  
772 fine-scale spatial pattern and heterogeneity of forest canopy structure: A lacunarity-based  
773 method designed for analysis of continuous canopy heights, *Forest Ecology and*  
774 *Management*, 214(1–3), 65–90, doi:10.1016/j.foreco.2005.03.056.

775 French, J. R. (2003), Airborne LiDAR in support of geomorphological and hydraulic modelling,  
776 *Earth Surface Processes and Landforms*, 28(3), 321–335, doi:10.1002/esp.484.

777 Glenn, N. F., D. R. Streutker, D. J. Chadwick, G. D. Thackray, and S. J. Dorsch (2006), Analysis  
778 of LiDAR-derived topographic information for characterizing and differentiating landslide  
779 morphology and activity, *Geomorphology*, 73(1–2), 131–148,  
780 doi:10.1016/j.geomorph.2005.07.006.

781 Glennie, C. L., A. Hinojosa-Corona, E. Nissen, A. Kusari, M. E. Oskin, J. R. Arrowsmith, and A.  
782 Borsa (2014), Optimization of legacy LiDAR data sets for measuring near-field earthquake  
783 displacements, *Geophysical Research Letters*, 41(10), 2014GL059919,  
784 doi:10.1002/2014GL059919.

785 Glennie, C. L., W. E. Carter, R. L. Shrestha, and W. E. Dietrich (2013), Geodetic imaging with  
786 airborne LiDAR: the Earth's surface revealed, *Rep. Prog. Phys.*, 76(8), 086801.

787 Guzzetti, F., A. C. Mondini, M. Cardinali, F. Fiorucci, M. Santangelo, and K.-T. Chang (2012),  
788 Landslide inventory maps: New tools for an old problem, *Earth Science Reviews*, 112(1–2),  
789 42–66, doi:10.1016/j.earscirev.2012.02.001.

790 Grünewald, T., M. Schirmer, R. Mott, and M. Lehning (2010). Spatial and temporal variability

791 of snow depth and SWE in a small mountain catchment, *The Cryosphere*, 4, 215-230,  
792 doi:10.5194/tc-4-215-2010

793 Hakala, T., J. Suomalainen, S. Kaasalainen, and Y. Chen (2012), Full waveform hyperspectral  
794 LiDAR for terrestrial laser scanning, *Opt. Express*, 20(7), 7119–7127,  
795 doi:10.1364/OE.20.007119.

796 Harman, C. J., K. A. Lohse, P. A. Troch, and M. Sivapalan (2014), Spatial patterns of vegetation,  
797 soils, and microtopography from terrestrial laser scanning on two semiarid hillslopes of  
798 contrasting lithology, *J. Geophys. Res. Biogeosci.*, 119(2), 163–180,  
799 doi:10.1002/2013JG002507.

800 Harpold, A. A. et al. (2014a), LiDAR-derived snowpack data sets from mixed conifer forests  
801 across the Western United States, *Water Resources Research*, 50(3), 2749–2755,  
802 doi:10.1002/2013WR013935.

803 Harpold, A. A., J. A. Biederman, K. Condon, M. Merino, Y. Korgaonkar, T. Nan, L. L. Sloat, M.  
804 Ross, and P. D. Brooks (2014b), Changes in snow accumulation and ablation following the  
805 Las Conchas Forest Fire, New Mexico, USA, *Ecohydrol.*, 7(2), 440–452,  
806 doi:10.1002/eco.1363.

807 Hartzell, P., C. Glennie, K. Biber, and S. Khan (2014), Application of multispectral LiDAR to  
808 automated virtual outcrop geology, *ISPRS Journal of Photogrammetry and Remote Sensing*,  
809 88(0), 147–155, doi:10.1016/j.isprsjprs.2013.12.004.

810 Hedrick, A., H. P. Marshall, A. Winstral, K. Elder, S. Yueh, and D. CLINE (2014), Independent  
811 evaluation of the SNODAS snow depth product using regional scale LiDAR-derived  
812 measurements, *The Cryosphere Discussions*, 8(3), 3141–3170, doi:10.5194/tcd-8-3141-  
813 2014.

814 Hopkinson, C., and M. N. Demuth (2006), Using airborne LiDAR to assess the influence of  
815 glacier downwasting on water resources in the Canadian Rocky Mountains, *Canadian*  
816 *Journal of Remote Sensing*, 32(2), 212–222, doi:10.5589/m06-012.

817 Hopkinson, C., J. Lovell, L. Chasmer, D. Jupp, N. Kljun, and E. van Gorsel (2013), Integrating  
818 terrestrial and airborne LiDAR to calibrate a 3D canopy model of effective leaf area index,  
819 *Remote Sensing of Environment*, 136(0), 301–314, doi:10.1016/j.rse.2013.05.012.

820 Hopkinson, C., T. Collins, A. Anderson, J. Pomeroy, and I. Spooner (2012), Spatial Snow Depth  
821 Assessment Using LiDAR Transect Samples and Public GIS Data Layers in the Elbow River

822 Watershed, Alberta, *Canadian Water Resources Journal*, 37(2), 69–87,  
823 doi:10.4296/cwrj3702893.

824 Hudak, A. T., E. K. Strand, L. A. Vierling, J. C. Byrne, J. U. H. Eitel, S. Martinuzzi, and M. J.  
825 Falkowski (2012), Quantifying aboveground forest carbon pools and fluxes from repeat  
826 LiDAR surveys, *Remote Sensing of Environment*, 123(0), 25–40,  
827 doi:10.1016/j.rse.2012.02.023.

828 Hurst, M. D., S. M. Mudd, K. Yoo, M. Attal, and R. Walcott (2013), Influence of lithology on  
829 hillslope morphology and response to tectonic forcing in the northern Sierra Nevada of  
830 California, *J. Geophys. Res. Earth Surf.*, 118(2), 832–851, doi:10.1002/jgrf.20049.

831 Hurst, M. D., S. M. Mudd, R. Walcott, M. Attal, and K. Yoo (2012), Using hilltop curvature to  
832 derive the spatial distribution of erosion rates, *Journal of Geophysical Research:*  
833 *Atmospheres (1984–2012)*, 117(F2), F02017, doi:10.1029/2011JF002057.

834 Hyde, P., R. Dubayah, B. Peterson, J. B. Blair, M. Hofton, C. Hunsaker, R. Knox, and W.  
835 Walker (2005), Mapping forest structure for wildlife habitat analysis using waveform  
836 LiDAR: Validation of montane ecosystems, *Remote Sensing of Environment*, 96(3–4), 427–  
837 437, doi:10.1016/j.rse.2005.03.005.

838 Hyypä, J., M. Holopainen, and H. Olsson (2012), Laser Scanning in Forests, *Remote Sensing*,  
839 4(10), 2919–2922, doi:10.3390/rs4102919.

840 James, L. A., M. B. Singer, S. Ghoshal, and M. Megison (2009), Historical channel changes in  
841 the lower Yuba and Feather Rivers, California: Long-term effects of contrasting river-  
842 management strategies, *Geological Society of America Special Papers*, 451, 57–81,  
843 doi:10.1130/2009.2451(04).

844 James, L. A., M. E. Hodgson, S. Ghoshal, and M. M. Latiolais (2012), Geomorphic change  
845 detection using historic maps and DEM differencing: The temporal dimension of geospatial  
846 analysis, *Geomorphology*, 137(1), 181–198, doi:10.1016/j.geomorph.2010.10.039.

847 Javernick, L., J. Brasington, and B. Caruso (2014), Modeling the topography of shallow braided  
848 rivers using Structure-from-Motion photogrammetry, *Geomorphology*, 213(0), 166–182,  
849 doi:10.1016/j.geomorph.2014.01.006.

850 Jencso, K. G., B.L. McGlynn, M.N. Gooseff, S.M. Wondzell, K.E. Bencala, and L.A. Marshall  
851 (2009), Hydrologic connectivity between landscapes and streams: Transferring reach-and  
852 plot-scale understanding to the catchment scale, *Water Resources Research*, 45(4), doi:

853 10.1029/2008WR007225

854 Jones, A. F., P. A. Brewer, E. Johnstone, and M. G. Macklin (2007), High-resolution  
855 interpretative geomorphological mapping of river valley environments using airborne  
856 LiDAR data, *Earth Surface Processes and Landforms*, 32(10), 1574–1592,  
857 doi:10.1002/esp.1505.

858 Kaasalainen, S., T. Lindroos, and J. Hyypä (2007), Toward Hyperspectral LiDAR:  
859 Measurement of Spectral Backscatter Intensity With a Supercontinuum Laser Source,  
860 *Geoscience and Remote Sensing Letters, IEEE*, 4(2), 211–215,  
861 doi:10.1109/LGRS.2006.888848.

862 Kampe, T. U., B.R. Johnson, M. Kuester, and M. Keller (2010), NEON: the first continental-  
863 scale ecological observatory with airborne remote sensing of vegetation canopy biochemistry  
864 and structure. *Journal of Applied Remote Sensing*, 4(1), 043510-043510, doi:  
865 10.1117/1.3361375

866 Khamsin, I., M. Zulkarnain, K. A. Razak, and S. Rizal (2014), Detection of tropical landslides  
867 using airborne LiDAR data and multi imagery: A case study in Genting highland, Pahang,  
868 *IOP Conference Series: Earth and Environmental Science*, 18(1), 012033.

869 Kessler, A. C., S. C. Gupta, H. A. S. Dolliver, and D. P. Thoma (2012), LiDAR Quantification of  
870 Bank Erosion in Blue Earth County, Minnesota, *Journal of Environmental Quality*, 41(1),  
871 197–207, doi:10.2134/jeq2011.0181.

872 Kinzel, P. J., C. J. Legleiter, and J. M. Nelson (2013), Mapping River Bathymetry With a Small  
873 Footprint Green LiDAR: Applications and Challenges<sup>1</sup>, *JAWRA Journal of the American*  
874 *Water Resources Association*, 49(1), 183–204, doi:10.1111/jawr.12008.

875 Kinzel, P. J., C. W. Wright, J. M. Nelson, and A. R. Burman (2007), Evaluation of an  
876 Experimental LiDAR for Surveying a Shallow, Braided, Sand-Bedded River, *Journal of*  
877 *Hydraulic Engineering*, 133(7), 838–842, doi:10.1061/(ASCE)0733-9429(2007)133:7(838).

878 Kirchner, P. B., R. C. Bales, N. P. Molotch, J. Flanagan, and Q. Guo (2014), LiDAR  
879 measurement of seasonal snow accumulation along an elevation gradient in the southern  
880 Sierra Nevada, California, *Hydrol. Earth Syst. Sci. Discuss.*, 11(5), 5327–5365,  
881 doi:10.5194/hessd-11-5327-2014.

882 Kohler, J., T. A. Neumann, J. W. Robbins, S. Tronstad, and G. Melland (2013), ICESat  
883 Elevations in Antarctica Along the 2007-09 Norway-USA Traverse: Validation With

884 Ground-Based GPS, *Geoscience and Remote Sensing, IEEE Transactions on*, 51(3), 1578–  
885 1587, doi:10.1109/TGRS.2012.2207963.

886 Krishnan, S., C. Crosby, V. Nandigam, M. Phan, C. Cowart, C. Baru, and R. Arrowsmith (2011),  
887 OpenTopography: A Services Oriented Architecture for Community Access to LIDAR  
888 Topography, pp. 7:1–7:8, ACM, New York, NY, USA.

889 Kurz, T. H., S. J. Buckley, J. A. Howell, and D. Schneider (2011), Integration of panoramic  
890 hyperspectral imaging with terrestrial LiDAR data, *The Photogrammetric Record*, 26(134),  
891 212–228, doi:10.1111/j.1477-9730.2011.00632.x.

892 Lague, D., N. Brodu, and J. Leroux (2013), Accurate 3D comparison of complex topography  
893 with terrestrial laser scanner: Application to the Rangitikei canyon (N-Z), *ISPRS Journal of*  
894 *Photogrammetry and Remote Sensing*, 82(0), 10–26, doi:10.1016/j.isprsjprs.2013.04.009.

895 Lam, N., M. Nathanson, N. Lundgren, R. Rehnström, and S.W. Lyon (2015), A Cost-Effective  
896 Laser Scanning Method for Mapping Stream Channel Geometry and Roughness, *Journal*  
897 *of the American Water Resources Association*, 1-10. DOI: 10.1111/1752-1688.12299.

898 Lane, S. N., C.J. Brookes, M.J. Kirkby, and J. Holden (2004), A network-index-based version of  
899 TOPMODEL for use with high-resolution digital topographic data, *Hydrological*  
900 *processes*, 18(1), 191-201, doi: 10.1002/hyp.5208.

901 Lane, C. R., and E. D’Amico (2010), Calculating the Ecosystem Service of Water Storage in  
902 Isolated Wetlands using LiDAR in North Central Florida, USA, *Wetlands*, 30(5), 967–977,  
903 doi:10.1007/s13157-010-0085-z.

904 Lee, H., K. C. Slatton, B. E. Roth, and W. P. Cropper (2009), Prediction of forest canopy light  
905 interception using three-dimensional airborne LiDAR data, *International Journal of*  
906 *Remote Sensing*, 30(1), 189–207, doi:10.1080/01431160802261171.

907 Lefsky, M. A., W. B. Cohen, G. G. Parker, and D. J. Harding (2002), Remote Sensing for  
908 Ecosystem Studies: LiDAR, an emerging remote sensing technology that directly measures  
909 the three-dimensional distribution of plant canopies, can accurately estimate vegetation  
910 structural attributes and should be of particular interest to forest, landscape, and global  
911 ecologists, *BioScience*, 52(1), 19–30, doi:10.1641/0006-  
912 3568(2002)052[0019:LRSFES]2.0.CO.

913 Legleiter, C. J., P. C. Kyriakidis, R. R. McDonald, and J. M. Nelson (2011), Effects of uncertain  
914 topographic input data on two-dimensional flow modeling in a gravel-bed river, *Water*

915 *Resources Research*, 47(3), W03518, doi:10.1029/2010WR009618.

916 Levy, J. S., A. G. Fountain, J. L. Dickson, J. W. Head, M. Okal, D. R. Marchant, and J. Watters  
917 (2013), Accelerated thermokarst formation in the McMurdo Dry Valleys, Antarctica, *Sci.*  
918 *Rep.*, 3, doi:10.1038/srep02269.

919 Li, S., R. A. MacMillan, D. A. Lobb, B. G. McConkey, A. Moulin, and W. R. Fraser (2011),  
920 LiDAR DEM error analyses and topographic depression identification in a hummocky  
921 landscape in the prairie region of Canada, *Geomorphology*, 129(3–4), 263–275,  
922 doi:10.1016/j.geomorph.2011.02.020.

923 Lin, Y., J. Hyypä, and A. Jaakkola (2011), Mini-UAV-Borne LIDAR for Fine-Scale Mapping,  
924 *Geoscience and Remote Sensing Letters, IEEE*, 8(3), 426–430,  
925 doi:10.1109/LGRS.2010.2079913.

926 Liu, Z. et al. (2008), CALIPSO LiDAR observations of the optical properties of Saharan dust: A  
927 case study of long-range transport, *Journal of Geophysical Research: Atmospheres (1984–*  
928 *2012)*, 113(D7), D07207, doi:10.1029/2007JD008878.

929 Lotsari, E., M. Vaaja, C. Flener, H. Kaartinen, A. Kukko, E. Kasvi, H. Hyypä, J. Hyypä, and  
930 P. Alho (2014), Annual bank and point bar morphodynamics of a meandering river  
931 determined by high-accuracy multitemporal laser scanning and flow data, *Water Resources*  
932 *Research*, 50, 5532–5559, doi:10.1002/2013WR014106.

933 Lyon, S.W., M. Nathanson, N. Lam, H.E. Dahlke, M. Rutzinger, J.W. Kean and H. Laudon  
934 (2015), Can Low-Resolution Airborne Laser Scanning Data Be Used to Model Stream  
935 Rating Curves?, *Water*, 7(4), 1324–1339, doi:10.3390/w7041324.

936 Mallet, C. and F. Bretar (2009). Full-waveform topographic LiDAR: State-of-the-art, *ISPRS*  
937 *Journal of Photogrammetry and Remote Sensing*, 64(1), 1–16, doi:  
938 10.1016/j.isprsjprs.2008.09.007.

939 Maltamo, M., E. Næsset, and J. Vauhkonen (Eds.) (2014), *Forestry Applications of Airborne*  
940 *Laser Scanning*, Springer, Netherlands.

941 Mandlbürger, G., C. Hauer, B. Höfle, H. Habersack, N. Pfeifer, others (2009), Optimisation of  
942 LiDAR derived terrain models for river flow modelling, *Hydrol. Earth Syst. Sci.*, 13(8),  
943 1453–1466, doi:10.5194/hess-13-1453-2009.

944 Mankoff, K. D., and T. A. Russo (2013), The Kinect: a low-cost, high-resolution, short-range 3D  
945 camera, *Earth Surface Processes and Landforms*, 38(9), 926–936, doi:10.1002/esp.3332.

946 Marks, K., and P. Bates (2000), Integration of high-resolution topographic data with floodplain  
947 flow models, *Hydrol. Process.*, *14*(11-12), 2109–2122, doi:10.1002/1099-  
948 1085(20000815/30)14:11/12<2109::AID-HYP58>3.0.CO;2-1.

949 Marshall, J. A., and J. J. Roering (2014), Diagenetic variation in the Oregon Coast Range:  
950 Implications for rock strength, soil production, hillslope form, and landscape evolution, *J.*  
951 *Geophys. Res. Earth Surf.*, *119*(6), 2013JF003004, doi:10.1002/2013JF003004.

952 Martinuzzi, S., L. A. Vierling, W. A. Gould, M. J. Falkowski, J. S. Evans, A. T. Hudak, and K.  
953 T. Vierling (2009), Mapping snags and understory shrubs for a LiDAR-based assessment of  
954 wildlife habitat suitability, *Remote Sensing of Environment*, *113*(12), 2533–2546,  
955 doi:10.1016/j.rse.2009.07.002.

956 Mascaro, J., M. Detto, G. P. Asner, and H. C. Muller-Landau (2011), Evaluating uncertainty in  
957 mapping forest carbon with airborne LiDAR, *Remote Sensing of Environment*, *115*(12),  
958 3770–3774, doi:10.1016/j.rse.2011.07.019.

959 Mason, D. C., D. M. Cobby, M. S. Horritt, and P. D. Bates (2003), Floodplain friction  
960 parameterization in two-dimensional river flood models using vegetation heights derived  
961 from airborne scanning laser altimetry, *Hydrol. Process.*, *17*(9), 1711–1732,  
962 doi:10.1002/hyp.1270.

963 Mattmann, C. A. (2013), Computing: A vision for data science, *Nature*, *493*(7433), 473-475,  
964 doi:10.1038/493473a

965 McCreight, J. L., A. G. Slater, H. P. Marshall, and B. Rajagopalan (2014), Inference and  
966 uncertainty of snow depth spatial distribution at the kilometre scale in the Colorado Rocky  
967 Mountains: the effects of sample size, random sampling, predictor quality, and validation  
968 procedures, *Hydrol. Process.*, *28*(3), 933–957, doi:10.1002/hyp.9618.

969 McKean, J. A., D. J. Isaak, and C. W. Wright (2008), Geomorphic controls on salmon nesting  
970 patterns described by a new, narrow-beam terrestrial–aquatic LiDAR, *Frontiers in Ecology*  
971 *and the Environment*, *6*(3), 125–130, doi:10.1890/070109.

972 McKean, J., D. Isaak, and W. Wright (2009), Improving stream studies with a small-footprint  
973 green LiDAR, *Eos, Transactions American Geophysical Union*, *90*(39), 341–342,  
974 doi:10.1029/2009EO390002.

975 McKean, J., D. Tonina, C. Bohn, and C. W. Wright (2014), Effects of bathymetric LiDAR errors  
976 on flow properties predicted with a multi-dimensional hydraulic model, *J. Geophys. Res.*

977 *Earth Surf.*, 119(3), 2013JF002897, doi:10.1002/2013JF002897.

978 Meyer, V., S. S. Saatchi, J. Chave, J. Dalling, S. Bohlman, G. A. Fricker, C. Robinson, and M.  
979 Neumann (2013), Detecting tropical forest biomass dynamics from repeated airborne LiDAR  
980 measurements, *Biogeosciences Discussions*, 10(2), 1957–1992, doi:10.5194/bgd-10-1957-  
981 2013.

982 Mitchell, P. J., P. N. J. Lane, and R. G. Benyon (2011), Capturing within catchment variation in  
983 evapotranspiration from montane forests using LiDAR canopy profiles with measured and  
984 modelled fluxes of water, *Ecohydrol.*, 5(6), 708–720, doi:10.1002/eco.255.

985 Moeser, D., J. Roubinek, P. Schleppei, F. Morsdorf, and T. Jonas (2014), Canopy closure, LAI  
986 and radiation transfer from airborne LiDAR synthetic images, *Agricultural and Forest*  
987 *Meteorology*, 197(0), 158–168, doi:10.1016/j.agrformet.2014.06.008.

988 Mora, B., M. A. Wulder, G. W. Hobart, J. C. White, C. W. Bater, F. A. Gougeon, A. Varhola,  
989 and N. C. Coops (2013), Forest inventory stand height estimates from very high spatial  
990 resolution satellite imagery calibrated with LiDAR plots, *International Journal of Remote*  
991 *Sensing*, 34(12), 4406–4424, doi:10.1080/01431161.2013.779041.

992 Mundt, J. T., D. R. Streutker, and N. F. Glenn (2006), Mapping Sagebrush Distribution Using  
993 Fusion of Hyperspectral and LiDAR Classifications, *Photogrammetric engineering and*  
994 *remote sensing*, 72(1), 47–54, doi:10.14358/PERS.72.1.47.

995 Musselman, K. N., S. A. Margulis, and N. P. Molotch (2013), Estimation of solar direct beam  
996 transmittance of conifer canopies from airborne LiDAR, *Remote Sensing of Environment*,  
997 136(0), 402–415, doi:10.1016/j.rse.2013.05.021.

998 Næsset, E. and T. Gobakken (2005). Estimating forest growth using canopy metrics derived from  
999 airborne laser scanner data, *Remote sensing of environment*, 96(3), 453-465, doi:  
1000 10.1016/j.rse.2005.04.001.

1001 Nathanson, M., J. W. Kean, T. J. Grabs, J. Seibert, H. Laudon, and S. W. Lyon (2012),  
1002 Modelling rating curves using remotely sensed LiDAR data, *Hydrol. Process.*, 26(9), 1427–  
1003 1434, doi:10.1002/hyp.9225.

1004 National Research Council (2012), *New Research Opportunities in the Earth Sciences*, National  
1005 Academy Press, Washington D.C.

1006 Nissen, E., T. Maruyama, J.R. Arrowsmith, J.R. Elliott, A.K. Krishnan, M.E. Oskin, and S.  
1007 Saripalli (2014), Coseismic fault zone deformation revealed with differential lidar: examples

1008 from Japanese Mw ~7 intraplate earthquakes, *Earth and Planetary Science Letters*, 405,  
1009 244-256, doi: doi:10.1016/j.epsl.2014.08.031.

1010 Nissen, E., A. K. Krishnan, J. R. Arrowsmith, and S. Saripalli (2012), Three-dimensional surface  
1011 displacements and rotations from differencing pre- and post-earthquake LiDAR point clouds,  
1012 *Geophysical Research Letters*, 39(16), L16301, doi:10.1029/2012GL052460.

1013 Olsoy, P. J., N. F. Glenn, P. E. Clark, and D. R. Derryberry (2014), Aboveground total and green  
1014 biomass of dryland shrub derived from terrestrial laser scanning, *ISPRS Journal of*  
1015 *Photogrammetry and Remote Sensing*, 88(0), 166–173, doi:10.1016/j.isprsjprs.2013.12.006.

1016 Oskin, M. E. et al. (2012), Near-Field Deformation from the El Mayor–Cucapah Earthquake  
1017 Revealed by Differential LIDAR, *Science*, 335(6069), 702–705,  
1018 doi:10.1126/science.1213778.

1019 Palminteri, S., G. V. N. Powell, G. P. Asner, and C. A. Peres (2012), LiDAR measurements of  
1020 canopy structure predict spatial distribution of a tropical mature forest primate, *Remote*  
1021 *Sensing of Environment*, 127(0), 98–105, doi:10.1016/j.rse.2012.08.014.

1022 Passalacqua, P., P. Tarolli, and E. Foufoula-Georgiou (2010), Testing space-scale methodologies  
1023 for automatic geomorphic feature extraction from LiDAR in a complex mountainous  
1024 landscape, *Water Resources Research*, 46(11), W11535, doi:10.1029/2009WR008812.

1025 Pelletier, J. D. (2013), Deviations from self-similarity in barchan form and flux: The case of the  
1026 Salton Sea dunes, California, *J. Geophys. Res. Earth Surf.*, 118(4), 2013JF002867,  
1027 doi:10.1002/2013JF002867.

1028 Pelletier, J. D. et al. (2013), Coevolution of nonlinear trends in vegetation, soils, and topography  
1029 with elevation and slope aspect: A case study in the sky islands of southern Arizona, *J.*  
1030 *Geophys. Res. Earth Surf.*, 118(2), 741–758, doi:10.1002/jgrf.20046.

1031 Pelletier, J. D., and C. A. Orem (2014), How do sediment yields from post-wildfire debris-laden  
1032 flows depend on terrain slope, soil burn severity class, and drainage basin area? Insights  
1033 from airborne-LiDAR change detection, *Earth Surface Processes and Landforms*, n/a–n/a,  
1034 doi:10.1002/esp.3570.

1035 Pelletier, J. D., and J. T. Perron (2012), Analytic solution for the morphology of a soil-mantled  
1036 valley undergoing steady headward growth: Validation using case studies in southeastern  
1037 Arizona, *Journal of Geophysical Research: Earth Surface (2003--2012)*, 117(F2),  
1038 doi:10.1029/2011JF002281.

1039 Pelletier, J. D., S. B. DeLong, C. A. Orem, P. Becerra, K. Compton, K. Gressett, J. Lyons-Baral,  
1040 L. A. McGuire, J. L. Molaro, and J. C. Spinler (2012), How do vegetation bands form in dry  
1041 lands? Insights from numerical modeling and field studies in southern Nevada, USA,  
1042 *Journal of Geophysical Research: Atmospheres (1984–2012)*, 117(F4), F04026,  
1043 doi:10.1029/2012JF002465.

1044 Perignon, M. C., G. E. Tucker, E. R. Griffin, and J. M. Friedman (2013), Effects of riparian  
1045 vegetation on topographic change during a large flood event, Rio Puerco, New Mexico,  
1046 USA, *J. Geophys. Res. Earth Surf.*, 118(3), 1193–1209, doi:10.1002/jgrf.20073.

1047 Perron, J. T., and J. L. Hamon (2012), Equilibrium form of horizontally retreating, soil-mantled  
1048 hillslopes: Model development and application to a groundwater sapping landscape, *Journal*  
1049 *of Geophysical Research: Atmospheres (1984–2012)*, 117(F1), F01027,  
1050 doi:10.1029/2011JF002139.

1051 Perron, J. T., J. W. Kirchner, and W. E. Dietrich (2008), Spectral signatures of characteristic  
1052 spatial scales and nonfractal structure in landscapes, *Journal of Geophysical Research:*  
1053 *Atmospheres (1984–2012)*, 113(F4), F04003, doi:10.1029/2007JF000866.

1054 Persson, A., A. Hasan, J. Tang, and P. Pilesjö (2012), Modelling Flow Routing in Permafrost  
1055 Landscapes with TWI: An Evaluation against Site-Specific Wetness Measurements,  
1056 *Transactions in GIS*, 16(5), 701–713, doi:10.1111/j.1467-9671.2012.01338.x.

1057 Plotnick, R. E., R. H. Gardner, W. W. Hargrove, K. Prestegard, and M. Perlmutter (1996),  
1058 Lacunarity analysis: A general technique for the analysis of spatial patterns, *Phys. Rev. E*,  
1059 53(5), 5461–5468, doi:10.1103/PhysRevE.53.5461.

1060 Rengers, F. K., and G. E. Tucker (2014), Analysis and modeling of gully headcut dynamics,  
1061 North American high plains, *J. Geophys. Res. Earth Surf.*, 119(5), 983–1003,  
1062 doi:10.1002/2013JF002962.

1063 Rhoades, E. L., M. A. O'Neal, and J. E. Pizzuto (2009), Quantifying bank erosion on the South  
1064 River from 1937 to 2005, and its importance in assessing Hg contamination, *Applied*  
1065 *Geography*, 29(1), 125–134, doi:10.1016/j.apgeog.2008.08.005.

1066 Riaño, D., F. Valladares, S. Condés, and E. Chuvieco (2004), Estimation of leaf area index and  
1067 covered ground from airborne laser scanner (LiDAR) in two contrasting forests, *Agricultural*  
1068 *and Forest Meteorology*, 124(3–4), 269–275, doi:10.1016/j.agrformet.2004.02.005.

1069 Richardson, J. J., L. M. Moskal, and S.-H. Kim (2009), Modeling approaches to estimate

1070 effective leaf area index from aerial discrete-return LIDAR, *Agricultural and Forest*  
1071 *Meteorology*, 149(6–7), 1152–1160, doi:10.1016/j.agrformet.2009.02.007.

1072 Roering, J. J. (2008), How well can hillslope evolution models “explain” topography?  
1073 Simulating soil transport and production with high-resolution topographic data, *Geological*  
1074 *Society of America Bulletin*, 120(9-10), 1248–1262, doi:10.1130/B26283.1.

1075 Roering, J. J., B. H. Mackey, J. A. Marshall, K. E. Sweeney, N. I. Deligne, A. M. Booth, A. L.  
1076 Handwerger, and C. Cerovski-Darriau (2013), “You are HERE”: Connecting the dots with  
1077 airborne LiDAR for geomorphic fieldwork, *Geomorphology*, 200(0), 172–183,  
1078 doi:10.1016/j.geomorph.2013.04.009.

1079 Roering, J. J., J. Marshall, A. M. Booth, M. Mort, and Q. Jin (2010), Evidence for biotic controls  
1080 on topography and soil production, *Earth and Planetary Science Letters*, 298(1–2), 183–190,  
1081 doi:10.1016/j.epsl.2010.07.040.

1082 Roering, J. J., L. L. Stimely, B. H. Mackey, and D. A. Schmidt (2009), Using DInSAR, airborne  
1083 LiDAR, and archival air photos to quantify landsliding and sediment transport, *Geophysical*  
1084 *Research Letters*, 36(19), L19402, doi:10.1029/2009GL040374.

1085 Sankey, J. B., D. J. Law, D. D. Breshears, S. M. Munson, and R. H. Webb (2013), Employing  
1086 LiDAR to detail vegetation canopy architecture for prediction of aeolian transport,  
1087 *Geophysical Research Letters*, 40(9), 1724–1728, doi:10.1002/grl.50356.

1088 Sankey, J. B., N. F. Glenn, M. J. Germino, A. I. N. Gironella, and G. D. Thackray (2010),  
1089 Relationships of aeolian erosion and deposition with LiDAR-derived landscape surface  
1090 roughness following wildfire, *Geomorphology*, 119(1–2), 135–145,  
1091 doi:10.1016/j.geomorph.2010.03.013.

1092 Schimel, D. S., G.P. Asner, and P. Moorcroft (2013), Observing changing ecological diversity in  
1093 the Anthropocene, *Frontiers in Ecology and the Environment*, 11(3), 129-137, doi:  
1094 10.1890/120111

1095 Seidel, D., S. Fleck, C. Leuschner, and T. Hammett (2011), Review of ground-based methods to  
1096 measure the distribution of biomass in forest canopies, *Annals of Forest Science*, 68(2), 225–  
1097 244, doi:10.1007/s13595-011-0040-z.

1098 Shook, K., J. W. Pomeroy, C. Spence, and L. Boychuk (2013), Storage dynamics simulations in  
1099 prairie wetland hydrology models: evaluation and parameterization, *Hydrol. Process.*,  
1100 27(13), 1875–1889, doi:10.1002/hyp.9867.

1101 Simard, M., N. Pinto, J. B. Fisher, and A. Baccini (2011), Mapping forest canopy height globally  
1102 with spaceborne LiDAR, *Journal of Geophysical Research: Atmospheres (1984–2012)*,  
1103 116(G4), G04021, doi:10.1029/2011JG001708.

1104 Snyder, N. P. (2009), Studying Stream Morphology With Airborne Laser Elevation Data, *Eos*,  
1105 *Transactions American Geophysical Union*, 90(6), 45–46, doi:10.1029/2009EO060001.

1106 Staley, D. M., T. A. Wasklewicz, and J. W. Kean (2014), Characterizing the primary material  
1107 sources and dominant erosional processes for post-fire debris-flow initiation in a headwater  
1108 basin using multi-temporal terrestrial laser scanning data, *Geomorphology*, 214(0), 324–338,  
1109 doi:10.1016/j.geomorph.2014.02.015.

1110 Stennett, T. A. (2004), LiDAR: Strap in tight, and prepare to go vertical, *Photogrammetric*  
1111 *engineering and remote sensing*, 70(5), 545–548.

1112 Stout, J. C., and P. Belmont (2014), TerEx Toolbox for semi-automated selection of fluvial  
1113 terrace and floodplain features from LiDAR, *Earth Surface Processes and Landforms*, 39(5),  
1114 569–580, doi:10.1002/esp.3464.

1115 Streutker, D. R., and N. F. Glenn (2006), LiDAR measurement of sagebrush steppe vegetation  
1116 heights, *Remote Sensing of Environment*, 102(1–2), 135–145, doi:10.1016/j.rse.2006.02.011.

1117 Sørensen, R., and J. Seibert (2007), Effects of DEM resolution on the calculation of  
1118 topographical indices: TWI and its components, *Journal of Hydrology*, 347(1–2), 79–89,  
1119 doi:10.1016/j.jhydrol.2007.09.001.

1120 Tarolli, P. (2014), High-resolution topography for understanding Earth surface processes:  
1121 Opportunities and challenges, *Geomorphology*, 216(0), 295–312,  
1122 doi:10.1016/j.geomorph.2014.03.008.

1123 Tenenbaum, D. E., L. E. Band, S. T. Kenworthy, and C. L. Tague (2006), Analysis of soil  
1124 moisture patterns in forested and suburban catchments in Baltimore, Maryland, using high-  
1125 resolution photogrammetric and LIDAR digital elevation datasets, *Hydrol. Process.*, 20(2),  
1126 219–240, doi:10.1002/hyp.5895.

1127 Thoma, D. P., S. C. Gupta, M. E. Bauer, and C. E. Kirchoff (2005), Airborne laser scanning for  
1128 riverbank erosion assessment, *Remote Sensing of Environment*, 95(4), 493–501,  
1129 doi:10.1016/j.rse.2005.01.012.

1130 Tinkham, W. T., A. M. S. Smith, H.-P. Marshall, T. E. Link, M. J. Falkowski, and A. H.  
1131 Winstral (2014), Quantifying spatial distribution of snow depth errors from LiDAR using

1132 Random Forest, *Remote Sensing of Environment*, 141(0), 105–115,  
1133 doi:10.1016/j.rse.2013.10.021.

1134 Trujillo, E., J. A. Ramírez, and K. J. Elder (2009), Scaling properties and spatial organization of  
1135 snow depth fields in sub-alpine forest and alpine tundra, *Hydrol. Process.*, 23(11), 1575–  
1136 1590, doi:10.1002/hyp.7270.

1137 Varhola, A., and N. C. Coops (2013), Estimation of watershed-level distributed forest structure  
1138 metrics relevant to hydrologic modeling using LiDAR and Landsat, *Journal of Hydrology*,  
1139 487(0), 70–86, doi:10.1016/j.jhydrol.2013.02.032.

1140 Varhola, A., N. C. Coops, Y. Alila, and M. Weiler (2014), Exploration of remotely sensed forest  
1141 structure and ultrasonic range sensor metrics to improve empirical snow models, *Hydrol.*  
1142 *Process.*, 28(15), 4433–4448, doi:10.1002/hyp.9952.

1143 Vierling, K. T., L. A. Vierling, W. A. Gould, S. Martinuzzi, and R. M. Clawges (2008), LiDAR:  
1144 shedding new light on habitat characterization and modeling, *Frontiers in Ecology and the*  
1145 *Environment*, 6(2), 90–98, doi:10.1890/070001.

1146 Vosselman, G., and H.-G. Maas (2010), *Airborne and terrestrial laser scanning*, CRC Press,  
1147 London.

1148 Wagner, W., M. Hollaus, C. Briese, and V. Ducic (2008), 3D vegetation mapping using small-  
1149 footprint full-waveform airborne laser scanners, *International Journal of Remote Sensing*,  
1150 29(5), 1433–1452, doi:10.1080/01431160701736398.

1151 Wallace, L., A. Lucieer, C. Watson, and D. Turner (2012), Development of a UAV-LiDAR  
1152 System with Application to Forest Inventory, *Remote Sensing*, 4(6), 1519–1543,  
1153 doi:10.3390/rs4061519.

1154 Wedding, L. M., A. M. Friedlander, M. McGranaghan, R. S. Yost, and M. E. Monaco (2008),  
1155 Using bathymetric LiDAR to define nearshore benthic habitat complexity: Implications for  
1156 management of reef fish assemblages in Hawaii, *Remote Sensing of Environment*, 112(11),  
1157 4159–4165, doi:10.1016/j.rse.2008.01.025.

1158 West, N., E. Kirby, P. Bierman, and B. A. Clarke (2014), Aspect-dependent variations in regolith  
1159 creep revealed by meteoric  $^{10}\text{Be}$ , *Geology*, 42(6), 507–510, doi:10.1130/G35357.1.

1160 Westoby, M. J., J. Brasington, N. F. Glasser, M. J. Hambrey, and J. M. Reynolds (2012),  
1161 “Structure-from-Motion” photogrammetry: A low-cost, effective tool for geoscience  
1162 applications, *Geomorphology*, 179(0), 300–314, doi:10.1016/j.geomorph.2012.08.021.

1163 Wheaton, J. M., J. Brasington, S. E. Darby, and D. A. Sear (2010), Accounting for uncertainty in  
1164 DEMs from repeat topographic surveys: improved sediment budgets, *Earth Surface*  
1165 *Processes and Landforms*, 35(2), 136–156, doi:10.1002/esp.1886.

1166 Williams, G. D. et al. (2013), Beyond Point Measurements: Sea Ice Floes Characterized in 3-D,  
1167 *Eos, Transactions American Geophysical Union*, 94(7), 69–70, doi:10.1002/2013EO070002.

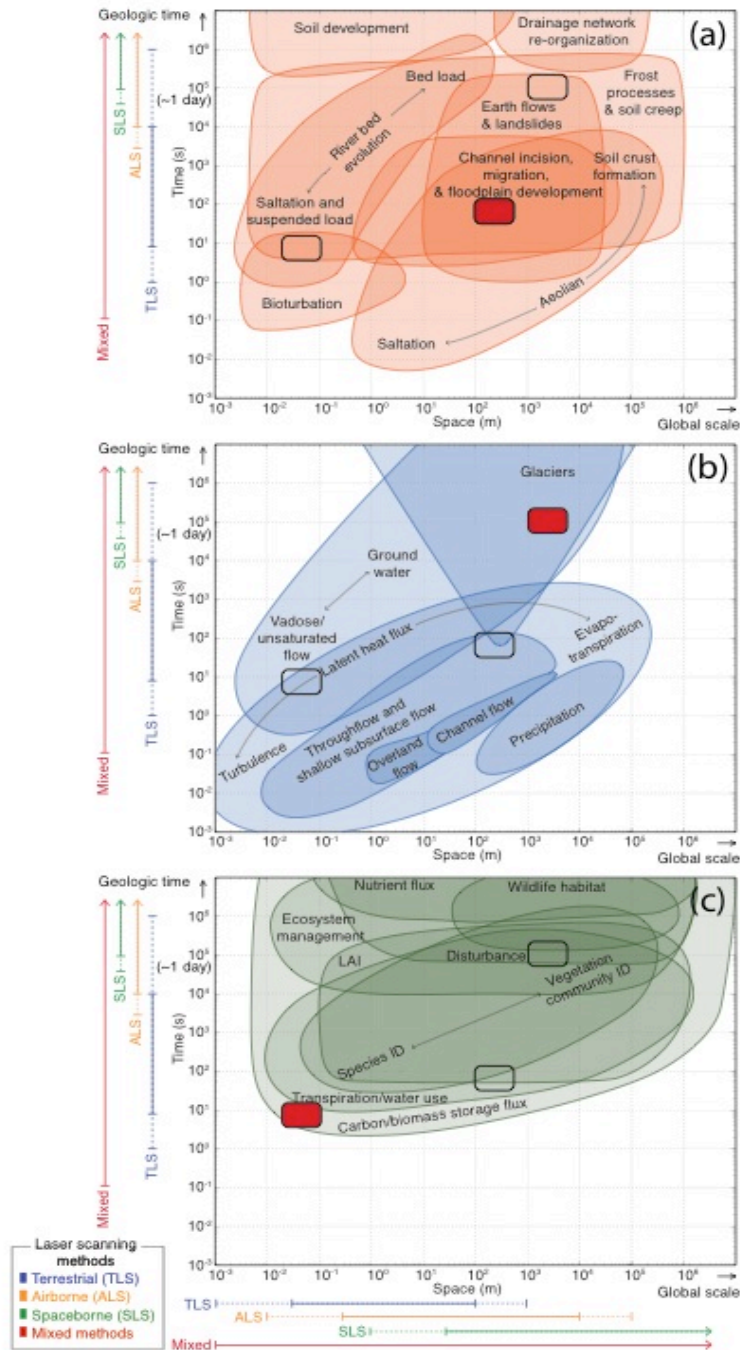
1168 Wulder, M. A., J. C. White, R. F. Nelson, E. Næsset, H. O. Ørka, N. C. Coops, T. Hilker, C. W.  
1169 Bater, and T. Gobakken (2012), LiDAR sampling for large-area forest characterization: A  
1170 review, *Remote Sensing of Environment*, 121(0), 196–209, doi:10.1016/j.rse.2012.02.001.

1171 Young, A. P., M. J. Olsen, N. Driscoll, R. E. Flick, R. Gutierrez, R. T. Guza, E. Johnstone, and  
1172 F. Kuester (2010), Comparison of Airborne and Terrestrial LiDAR Estimates of Seacliff  
1173 Erosion in Southern California, *Photogrammetric engineering and remote sensing*, 76(4),  
1174 421–427, doi:10.14358/PERS.76.4.421.

1175 Yu, X., J. Hyyppä, H. Kaartinen, and M. Maltamo (2004), Automatic detection of harvested trees  
1176 and determination of forest growth using airborne laser scanning, *Remote Sensing of*  
1177 *Environment*, 90(4), 451–462, doi:10.1016/j.rse.2004.02.001.

1178 Zellweger, F., F. Morsdorf, R. Purves, V. Braunisch, and K. Bollmann (2014), Improved  
1179 methods for measuring forest landscape structure: LiDAR complements field-based habitat  
1180 assessment, *Biodivers Conserv*, 23(2), 289–307, doi:10.1007/s10531-013-0600-7.

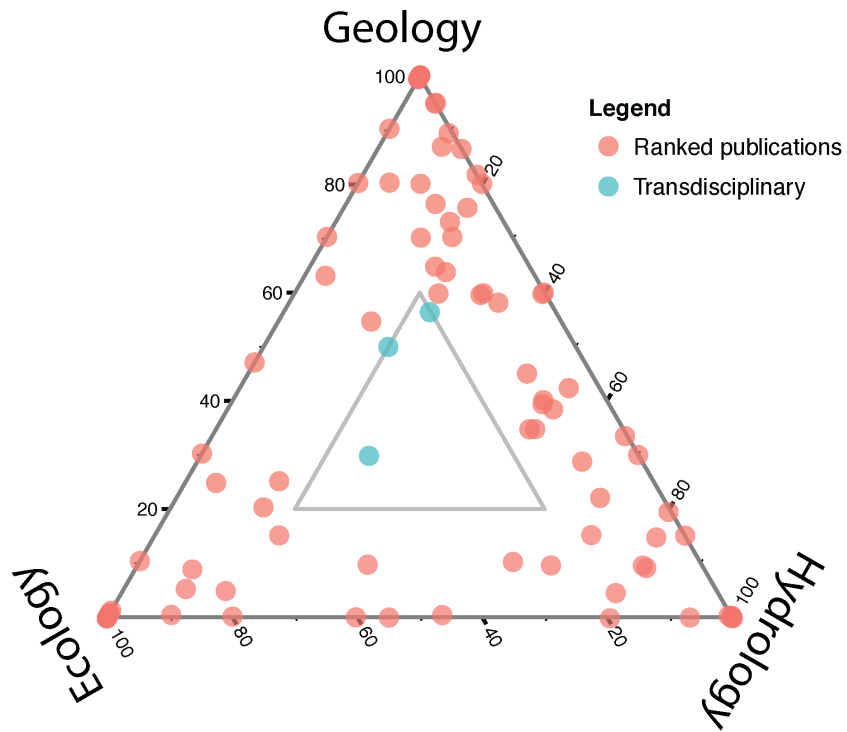
1181 Zhao, K., S. Popescu, and R. Nelson (2009), LiDAR remote sensing of forest biomass: A scale-  
1182 invariant estimation approach using airborne lasers, *Remote Sensing of Environment*, 113(1),  
1183 182–196, doi:10.1016/j.rse.2008.09.009.



1184

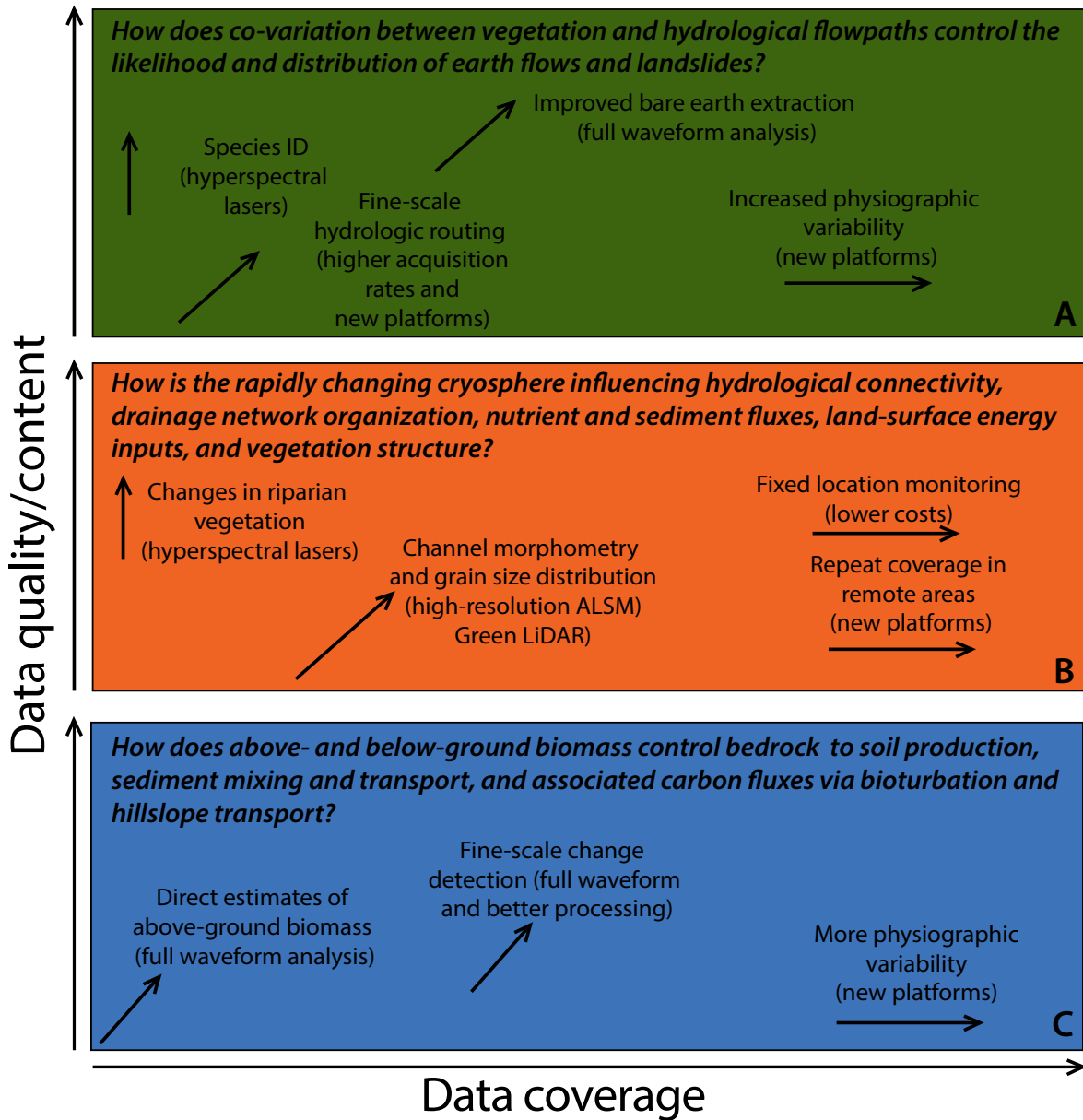
1185 **Figure 1.** Important CZ processes graphed as a function of time versus space for geomorphology  
 1186 (a), hydrology (b), and ecology (c). The spatial and temporal scales that lidar is currently  
 1187 addressing are shown as colored bars, with dotted bars indicating increasing resolutions and  
 1188 larger extents available in the next five years. Overlapping spatiotemporal scales that encompass  
 1189 the example questions in the Figure 3 are also noted with red boxes.

1190



1191  
 1192  
 1193  
 1194  
 1195  
 1196  
 1197  
 1198

**Figure 2.** Depiction of the disciplinary focus of 147 journal articles using lidar. Articles were qualitatively ranked based on their applicability to geomorphological, hydrological, and/or ecological process understanding. Articles in the center are examples of transdisciplinary lidar applications, with those shown in blue used as exemplars in the text.



1199  
 1200  
 1201  
 1202  
 1203  
 1204  
 1205  
 1206  
 1207

**Figure 3.** Example CZ research questions conceptualizing the transdisciplinary potential of lidar datasets when coupled with future technological advances. The questions encompass processes from geomorphology (a), hydrology (b), and ecology (c) that overlap spatial and temporal scales. These scales are noted in Figure 1. The text in the panel notes specific improvements offered and the technology needed in parentheses. The arrows qualitatively represent whether the technological advance expands data coverage and/or data quality/content.